Title
Investigation of surface properties of quince seed extract as a novel polymeric surfactant

Authors
Kirtil, Emrah
Svitova, Tatyana
Radke, Clayton J
et al.

Publication Date
2022-02-01

DOI
10.1016/j.foodhyd.2021.107185

Peer reviewed

Food Hydrocolloids 123 (2022) 107185

Contents lists available at ScienceDirect

Food Hydrocolloids

journal homepage: www.elsevier.com/locate/foodhyd

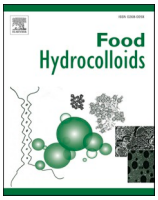

Investigation of surface properties of quince seed extract as a novel polymeric surfactant

Emrah Kirtil [a,b,c,*], Tatyana Svitova [a], Clayton J. Radke [a], Mecit Halil Oztop [b], Serpil Sahin [b]

[a] Chemical and Biomolecular Engineering Department, University of California Berkeley, 101E Gilman, Berkeley, CA, 94720-1462, USA
[b] Department of Food Engineering, Middle East Technical University, 06800, Ankara, Turkey
[c] Food Engineering Department, Yeditepe University, 34755, Kayisdagi, Istanbul, Turkey

ARTICLE INFO

Keywords:
Quince seed extract
Surface tension
Surface rheology
Hydrocolloids
Adsorption
Polymeric surfactant

ABSTRACT

In recent years, there is a growing trend from both academia and the industry towards the use of "clean-labeled" ingredients obtained from renewable resources. Proteins and polysaccharides, in particular, are becoming increasingly popular as alternatives to already well-established synthetic surfactants. Quince seeds are a relatively novel hydrocolloid source that has recently raised interest among researchers due to their strong surface activity and viscosity-enhancing properties. This study investigates quince seed extract's surface properties (dynamic surface tension and dilatational surface rheology) and how they differ with varying concentrations (between 0.01% and 1%), pH's (3, 7, 9, and 11), and ionic strengths (0.1, 0.3, 0.5 M NaCl). By QSE addition alone, equilibrium surface tension could be lowered to ~36 mN/m, which is lower than the lowest ST that can be achieved with many other surface active biopolymers. Critical aggregation concentration (CAC) was identified as 0.165% w/v, meaning a relatively low extract concentration was sufficient to provide complete surface coverage. Dynamic surface tension curves revealed almost instantaneous polymer adsorption for concentrations over 0.01% w/v, which demonstrates the strong potential of the gum as a foaming agent. As solution pHs get further from the isoelectric point of QSE proteins, the rate of adsorption of QSE molecules onto the interface and the equilibrium surface pressures increased. Surface properties were also significantly affected by the ionic strength of the medium, with eq. STs decreasing with increasing QSE concentration. pH and ionic strength induced conformational changes in the interfacial layer and also led to local minima and maxima in dilatational elastic and loss modulus within ranges studied. Considering these findings, QSE is a very promising natural alternative to other polymeric surfactants and stabilizers currently used in the food, cosmetic and pharmaceutical industries.

1. Introduction

In recent years, there is a growing trend from both the academia and the industry towards the use of "clean-labeled" ingredients obtained from renewable resources. Biopolymers are being used for their stabilizing, emulsifying, viscosity-enhancing, micro-encapsulating, and gelling properties, among others (Farahmandfar et al., 2017). Proteins and polysaccharides, in particular, are becoming increasingly popular as alternatives to already well-established synthetic surfactants (Bouyer et al., 2012; Covis et al., 2014; Dalgleish, 2006; Dickinson, 2003). In addition to their environmental impact, synthetic surfactants may cause acute toxic symptoms in animals and humans (Cserháti et al., 2002; Effendy & Maibach, 1995; Liwarska-Bizukojc et al., 2005). Thus, replacing them with much safer alternatives would be of significant benefit.

Proteins are adsorbing biopolymers; that is, they adsorb to the interface, decreasing surface tension, and easing the emulsification process. Even though proteins, compared to low molecular weight surfactants, adsorb more slowly to the interface; during emulsification process, where turbulent hydrodynamic conditions are present, they can adsorb quite rapidly (Seta et al., 2014; W.; Wang, Zhou, et al., 2014). Once adsorbed, these polymers with their high molecular weight and complex structure form a highly viscoelastic gel layer on the interface which provides an additional layer of protection to droplet coalescence during subsequent processing and storage (Benjamins et al., 1996; Bos & Van Vliet, 2001; Dickinson, 1998, 1999, 2001). Non-adsorbing polysaccharides, on the other hand, contribute to dispersion stability by forming an extended network in the continuous phase that enhances its

* Corresponding author. Food Engineering Department, Yeditepe University, 34755, Kayisdagi, Istanbul, Turkey.
E-mail address: emrah.kirtil@yeditepe.edu.tr (E. Kirtil).

https://doi.org/10.1016/j.foodhyd.2021.107185
Received 27 December 2020; Received in revised form 7 September 2021; Accepted 8 September 2021
Available online 17 September 2021

viscosity, even create a gel, thus hindering droplet movements and encounters (Bouyer et al., 2013). Merging the advantages of proteins (interfacial adsorption, reduction in interfacial tension) and polysaccharides (steric repulsion, viscosity enhancement) in the same system, and coming up with the most appropriate conditions (concentration, pH, ionic strength, temperature) to increase their stabilizing properties, poses a great potential in improving dispersion stability (Dickinson, 2008a, 2008b; Evans et al., 2013; Guzey & McClements, 2006).

Various strategies have been developed for this purpose. One common approach involves the chemical modification of biopolymers' native structure. By dry heating of protein and polysaccharides, amino group in proteins become covalently attached to the carbonyl group of a reducing end on the polysaccharide backbone through *Maillard* reaction (Anal et al., 2019; Kontogiorgos, 2019a). In systems stabilized by such biopolymers, the protein can first adsorb at the interface. Polysaccharides linked to the proteins extend from the interface to the bulk phase and provide steric stabilization. Systems stabilized by this approach have shown enhanced kinetic stability compared to systems stabilized by proteins and polysaccharides alone or in combinations (Anal et al., 2019; Bouyer et al., 2013; Gao et al., 2017; Liu et al., 2018; Vernon-Carter et al., 2008). Several natural gums possess this exceptional attribute in their native state. Out of these, gum Arabic is the most widely used adsorbing biopolymer and is considered a benchmark emulsifying, encapsulating, and film-forming agent (Vernon-Carter et al., 2008). Gum Arabic is an extensively branched complex heteropolyelectrolyte composed of L-arabinose and D-galactose and minor proportions of 4-O-methyl-D-glucuronate L-rhamnose. The gum's surface-activity comes from its protein content (1–2% w/w) (Goycoolea et al., 1997; Orozco-Villafuerte et al., 2003; Ray et al., 1995). However, the use of this gum is restricted by its high cost (Dickinson, 2018).

Quince seed extract has shown similar characteristics to Gum Arabic and, thus, has raised some interest among researchers. Quince (scientific name *Cydonia oblonga*) is a fruit native to the West Asian region, and its cultivation is especially high in Caucasus regions, Iran, Afghanistan, Dagestan, and Antalya (Abbastabar et al., 2015). The fruit seed mucilage is composed of three polysaccharide fractions, with the major fraction being a graft copolymer with a molecular weight of 1.4×10^6 Da. This major fraction consists of (1/4)-linked and (1/2, 4)-linked xylopyranosyl residues at the backbone with glucuronic acid and arabinose units forming the branches (L. Wang et al., 2018). The soluble protein content varies between 11% and 25% depending on the pH (Ritzoulis et al., 2014). The seed extract has shown very high emulsification and foaming properties (Deng et al., 2019). This is related to its high hydrophobic amino acid content, which gives the hydrocolloid exceptional surface activity (Deng et al., 2019). However, research up until now has concentrated mainly on the chemical and physical analysis of quince seed mucilage's water-soluble carbohydrates. There still is a considerable amount of research needed to examine the gum's potential in stabilizing dispersions, such as investigation of its surface properties and use of the gum in a real dispersed system.

In analysis of a surface-active material, a comprehensive understanding of the adsorption mechanism is crucial in determining its functionality. These involve, but not limited to, foaming and emulsification applications that are widely employed in the production of pharmaceuticals, cosmetics, and foods, as well as mining and oil industry (Karbaschi et al., 2014). In addition to industrial applications, examination of the dynamics of interfacial layers is also critical from a fundamental point of view as it generates the possibility of understanding the interaction of molecules, change in their conformations, and the process of molecular aggregation formation (Karbaschi et al., 2014). In literature, for years, there have been many studies on surfactant equilibrium adsorption properties (i.e., adsorption isotherms). With the increasing availability of modern technologies, advanced investigations dedicated to adsorption kinetics, interfacial viscoelastic behavior, and changes of the interfacial electric charge are becoming possible (Möbius et al., 2001).

As proteins adsorb to an oil/water interface, changes occurring in interfacial properties are an indication of the individual sub-processes at play (Beverung et al., 1999). These examinations are conducted by a variety of complicated scientific instruments (Arabadzhieva et al., 2011). Out of these, interfacial tension remains the most straightforward and accessible dynamic quantity of a fluid interface. This method features the formation of a fresh interface and the subsequent determination of interfacial tension as a function of time (Karbaschi et al., 2014). Surface-active molecules, as they adsorb to the interface, decrease the interfacial tension, facilitating the dispersion of two phases within one another. This is explained by a reduction in Gibbs' free energy of system (W. Wang, Zhou, et al., 2014). This process though simple in principle, provides data related to both the state and denseness of the interfacial layers and the surfactant exchange between the interface and solution bulk, as well as the stability of the dispersion (Arabadzhieva et al., 2011; Benjamins et al., 1996; Liggieri et al., 2002; Ravera et al., 2005; Senkel et al., 1998).

However, reduced interfacial tension is not the only parameter that governs stability. Kinetically stabilized emulsions by large molecule surfactants were demonstrated to remain stable for years, despite having an interfacial tension of around 30–40 mN/m; whereas emulsions formed by certain lower paraffin hydrocarbons do not remain stable even when the interfacial tension is extremely low (W. Wang, Zhou, et al., 2014). Emulsion and foam stability have been associated with interfacial skin formation, which refers to the generation of a gel-like network and is more dominantly observed in interfacial adsorption of macromolecular species (Erik M. Freer et al., 2004b). This means equal surface forces do not essentially mean equal foam or emulsion stabilities. Thus, it would be wrong to explain the stability of dispersions solely by the magnitude of repulsive interactions acting normal to the film surface. There happens to be another factor that plays a role in dampening external disturbances, hence preventing film rupture. The barriers against coalescence are thin liquid films, attributes of which are governed by interfacial rheological properties of the respective surfactant layer (Santini et al., 2007).

The dilatational surface rheology method is based on applying periodic expansion and contraction to the interface with subsequent measurement of the change in interfacial tension as a response to these perturbations (Miller et al., 1996). This methodology gives information on the interface's resistance to deformation. When the dispersion consists of two (or more) fluid phases in particular, the deformation of one material implies a deformation of all the constitutive phases. As such, dilatational rheology measurements give us an insight on the stability of dispersed system against disturbances it could infer during formation, processing (such as spraying and atomization), and storage (Rodríguez Patino & Rodríguez Niño, 1999). Additionally, unlike surface tension which operates normal to the surface, interfacial dilatational elasticity is associated with forces that act tangentially to the surface (Santini et al., 2007). There is a multitude of studies in the literature that have demonstrated a correlation between surface dilatational properties and stability of dispersed systems (Cao et al., 2013; Davis & Foegeding, 2006; Langevin, 2000; Stubenrauch & Miller, 2004; Tadros, 2009; Vernon-Carter et al., 2008; Zhang et al., 2011).

This study focuses on quince seed extract's air/water interfacial properties to represent how the extract would behave in an actual foam application. Foams are dispersions obtained by gas incorporation into a continuous matrix of solid or liquid. Most of the studies on foams are carried out on wet foams, as they are thermodynamically unstable. Their large interfacial area makes them very prone to destabilization, mainly through the processes of drainage, coalescence, and Oswalt ripening (Gonzenbach et al., 2007; Tcholakova et al., 2011). To slow down these processes, surface-active species are used. Any material adsorbing on the foam surface, providing elasticity to the thin interfacial film layer, contributes to foam's kinetic stability. In particular, the presence of polymer-based surfactants might act as a gelling or crosslinking agent

through irreversible adsorption to the interface. This allows the formation of a stable three-dimensional foam network of interconnected bubbles, which significantly prevents foam collapse (Zabiegaj et al., 2013).

Even though first studies on quince seed extract dates back to 1930s (Renfrew & Cretcher, 1932), and there have been several exciting findings (de Escalada Pla et al., 2010; Rakhimov et al., 1985), it is safe to say that this seed with exceptional properties has not received enough attention. To best our knowledge, there are currently no studies examining the surface properties of this extract or its potential application in a wet foam system. Knowing the material used is essential in making sense of microstructural changes occurring on the interface. Hence, we believed this manuscript would not be complete without some supplementary information (in Appendix), which summarizes the very few literature studies on the extract's chemical and physicochemical properties. We strongly suggest that the readers with no prior knowledge of the material go over this literature review (Section A1) before moving on to the results and discussion.

This study aims to establish how the extract's surface properties (dynamic surface tension and dilatational surface rheology) differ with varying concentrations (between 0.01% and 1%), pH's (3, 7, 9, and 11), and ionic strengths (0.1, 0.3, 0.5 M NaCl). This way, in a fundamental point of view; the study provides the possibility of gaining more information on the processes occurring during adsorption and explaining their mechanism with established theories; as well as, providing the readers with direct information of this extract's application and it is performance as a stability enhancer in foams.

2. Material & methods

2.1. Materials

Quince seed extract (QSE) was obtained from seeds of the quinces purchased from a local grocery store during the winter season in Ankara, Turkey. All solutions were prepared with distilled water further purified using a Milli-Q filtration unit (with a resistivity $\geq$18.2 MΩ cm) (Millipore Co., Bedford, WA). The pH and ionic strength of the solutions were adjusted using HCl (0.1 M at pH1), NaOH (0.1 M at pH13) and NaCl purchased from Sigma-Aldrich Chemie Gmbh (Darmstadt, Germany).

Table 1
Experimental design.

Sample name	Concentration of QSE (% w/v)	pH	NaCl Concentration (M)
Q0.01	0.01	7	0
Q0.025	0.025	7	0
Q0.05	0.05	7	0
Q0.1	0.1	7	0
Q0.15	0.15	7	0
Q0.175	0.175	7	0
Q0.185	0.185	7	0
Q0.2	0.2	7	0
Q0.3	0.3	7	0
Q0.4	0.4	7	0
Q0.5	0.5	7	0
Q0.6	0.6	7	0
Q0.75	0.75	7	0
Q1	1	7	0
P3	0.3	3	0
P7	0.3	7	0
P11	0.3	11	0
S0	0.3	7	0
S0.1	0.3	7	0.1
S0.3	0.3	7	0.3
S0.5	0.3	7	0.5

2.2. Methods

2.2.1. Experimental design

The experimental design followed is given in Table 1.

Surface-active polymer concentration is one of the most influential factors in determining the system's interfacial properties. Therefore, a wide range of concentrations was investigated. After preliminary trials, the bottom limit was decided as 0.01% (w/v), which is the least amount of polymer that has a notable effect on lowering surface tension. The upper range was chosen as 1% (w/v) since, after this concentration, the viscosity of the solutions was exceedingly high, which is known to hinder the effects of surface relaxation due to molecular diffusion (Pérez-Mosqueda et al., 2013). The concentration span between two consecutive concentrations were narrowed down, getting closer to the identified critical aggregation concentration (CAC = 0.165% w/v). This was done to identify CAC and further examine the properties of the solution at that point.

At a set concentration, the fate of the polysaccharide at the air-water surface, hence the stability of the dispersions, is a function of its molecular characteristics and water-air-polymer interactions. Hydrocolloid conformation plays a vital role in that regard (Kontogiorgos, 2019). Hydrocolloids dispersed in food systems that can display a wide range of pHs and ionic strengths similarly can exhibit exceptionally different molecular conformations. Thus, we have prepared solutions with a set amount of QSE (0.3% w/v) and changed pH (3, 7, and 11) and NaCl concentration (0, 0.1, 0.3, and 0.5 M).

2.2.2. Quince seed extract preparation

A modified version of the method by Abbastabar et al. (2015) was followed to gather the extract of quince seeds. Seeds were separated from the fruit flesh and freeze-dried. The seeds were then ground before being soaked into deionized water. Aqueous ground seed mixture (with a water/solid ratio of 50:1) was continuously stirred with a magnetic stirrer at 25 °C for 24 h. The resulting suspension was centrifuged (at 10, 000 rpm for 30 min) and filtered with a cheesecloth. The aqueous solution acquired was freeze-dried to obtain crude gum extract. The method yielded approximately 8% extract, based on the dry weight of seeds.

2.2.3. Sample preparation

Pre-determined amounts of QSE were added to Millipore water with pH adjusted (to either 3, 7 or 11), and solutions were mixed with a magnetic stirrer for 3 h before measurements. QSE was acidic in nature, so a final adjustment was performed after QSE addition to secure the set pHs. For adjustment of ionic strength of solutions, NaCl was added to Millipore water (pH7) in given amounts to obtain solutions of 0.1, 0.3, and 0.5 M.

2.2.4. Dynamic surface tension

A Ramé-Hart tensiometer (Ramé-Hart Instrument Co., Netcong, NJ, USA) coupled with an automated dispenser was used for real-time surface tension data acquisition. The droplet profile was recorded through a charge-coupled device camera and digitized via a computer with DropImage Advanced software, v.2.2. installed. A schematic of the system is given in Fig. 1.

Prior to measurements, the system was calibrated by a 4 mm diameter spherical standard. Additionally, in-between measurements, syringe and needle were cleaned with ethanol solution followed by an abundant rinse with MilliQ water. The cleanliness of the water and the equipment was ensured by the measurement of surface tension of MilliQ water. Measurements were pursued if water yielded a constant ST profile at 72 $\pm$ 0.5 mN/m for 10 min. Data points were taken each 30 s. The automated pipette system was adjusted to maintain drop volumes constant at 25 μL.

Pendant drop technique was employed for surface tension measurements. This technique involves the calculation of surface tension

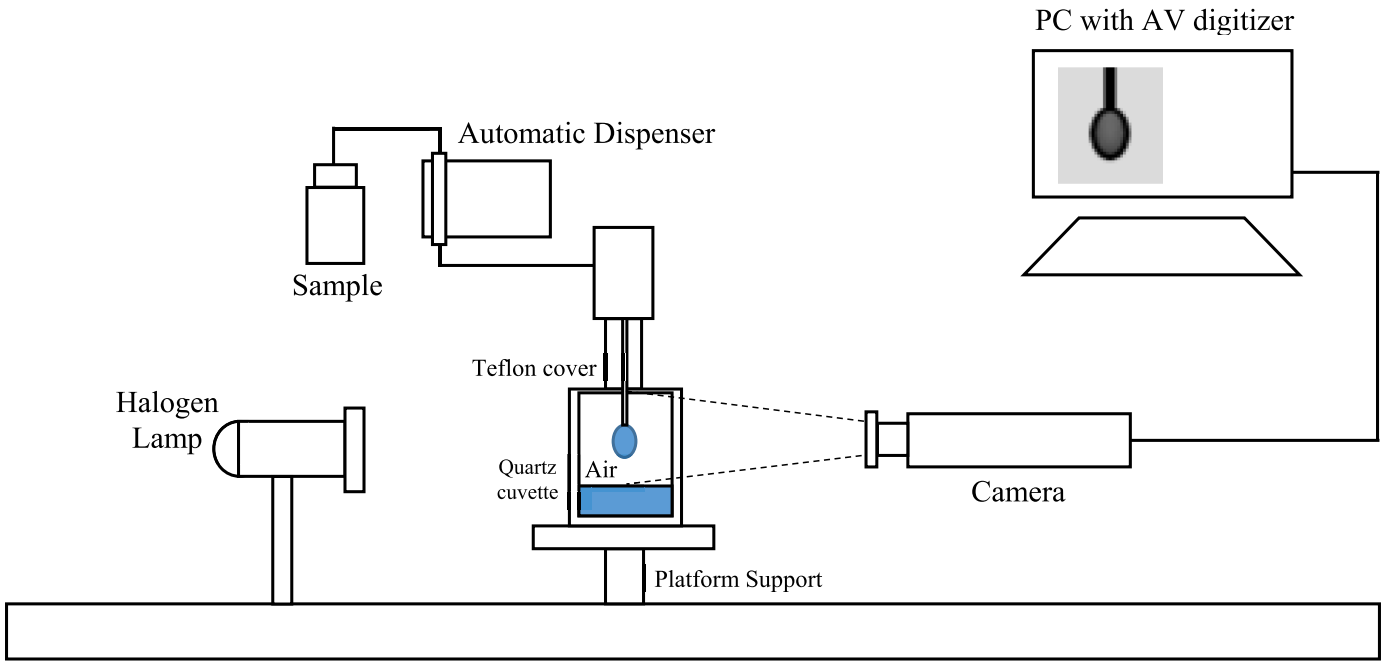

Fig. 1. Schematic representation of the pendant drop measurement setup.

from the size and the vertical shape of a drop left hanging under the effect of gravity from the tip of a needle inside a secondary fluid phase (which was air in our case). The needle was connected to a syringe, which was controlled by computer software. Computer automation enables rapid drop image acquisition, edge detection, and fitting of the axisymmetric drop shape to the Young-Laplace equation to find the surface tension. The basic principle of the measurement is based on the variation in pressure across a surface. The two areas of curvature of the surface and surface tension are related to this pressure difference by Young-Laplace equation (Eqn. (1)).

$$\Delta P = \gamma\left(\frac{1}{R_1}+\frac{1}{R_2}\right) \tag{1}$$

where ΔP is Laplace pressure (the pressure difference across fluid interface), γ is the surface tension, R_1 and R_2 are the orthogonal maximum curvature radii of the elongated drop (Berry et al., 2015; W.; Wang, Zhou, et al., 2014). The drop profiles were continuously monitored; hence the reduction in surface tension could be recorded as a function of time.

To distinguish the drop from any outside effects, the tip of the needle was positioned inside a thermostatized quartz cuvette at 25 °C. To keep relative humidity constant inside; the cell was covered with waxed Teflon lids (Fig. 1). In order to prevent droplet shrinkage due to evaporation, the cell was filled with 2 ml distilled water. However, even in a saturated atmosphere, monitoring a single droplet over long periods is limited by evaporation or adsorption effects (Erik M. Freer et al., 2004b; Wüstneck et al., 1996). Evaporation causes a reduction in surface area, which causes compression and changes in polymer density at the surface.

Multiple researchers claimed that it is impossible to identify large surface-active polymers' real equilibrium (such as proteins). After positioning themselves to the sub-surface (the hypothetical layer right beneath the interface), these large molecules continue to reorient themselves to develop the most compact and practical conformation that minimizes surface free energy (Beverung et al., 1999; Ward & Tordai, 1946). This procedure might continue even after 24 h (Arabadzhieva et al., 2011; Beverung et al., 1999). However, as previously mentioned, prolonged observation of the same drop is subject to errors due to water evaporation/adsorption effects. For this reason, specimens were subjected to a detailed analysis with a high number of replications for varying periods. All samples were monitored for 24 h at least twice. Depending on these results, we believed reliable dynamic surface tension data could only be taken within the first 2 h. Hence, the remaining replicates were monitored for 60–120 min. Due to the large and complex molecular structure of the QSE, relaxation profiles turned out to be quite complicated, and repeatability was rather low. To ensure data reliability, the total number of replicates varied between 8 and 10. A two-way analysis of variance was performed (with $\alpha = 0.05$).

Within the first 120 min, true adsorption equilibrium, if it really exists, could not be reached. Nevertheless, after a period of 30–60 min, all samples displayed a pseudo-equilibrium where the tension did not change by more than 1 mN/m in 1 h. Equilibrium surface tension data reported (in Fig. 2) are actually these pseudo-equilibrium values. Similar behavior was observed by various researcher studying surface behavior of proteins, and a similar approach was followed (Bouyer et al., 2013; Cao et al., 2013; Sosa-Herrera et al., 2016; Vereyken et al., 2001; Wüstneck et al., 1996).

2.2.5. Surface rheology

2.2.5.1. Theoretical background. Equilibrium surface tension analysis and the rate of surface tension relaxation provide information on the surface coverage mechanism. However, viscoelasticity of the interfaces after dilation/compression or shear, being much more sensitive to disturbances in the adsorption layer, gives access to a broader range of information that is not attainable with surface tension analysis only (Karbaschi et al., 2014).

In this method, the drop is subjected to a sinusoidal expansion and contraction at a set oscillation frequency. A similar change in surface tension accompanies this infinitesimal periodic change in area. The dilatational surface modulus (ε) is defined as the change in surface tension (γ) with a change in surface area (A) (Lucassen & Van Den Tempel, 1972a).

$$E = \frac{d\gamma}{dA} \tag{2}$$

There are two contributions to dilatational modulus; dilatational

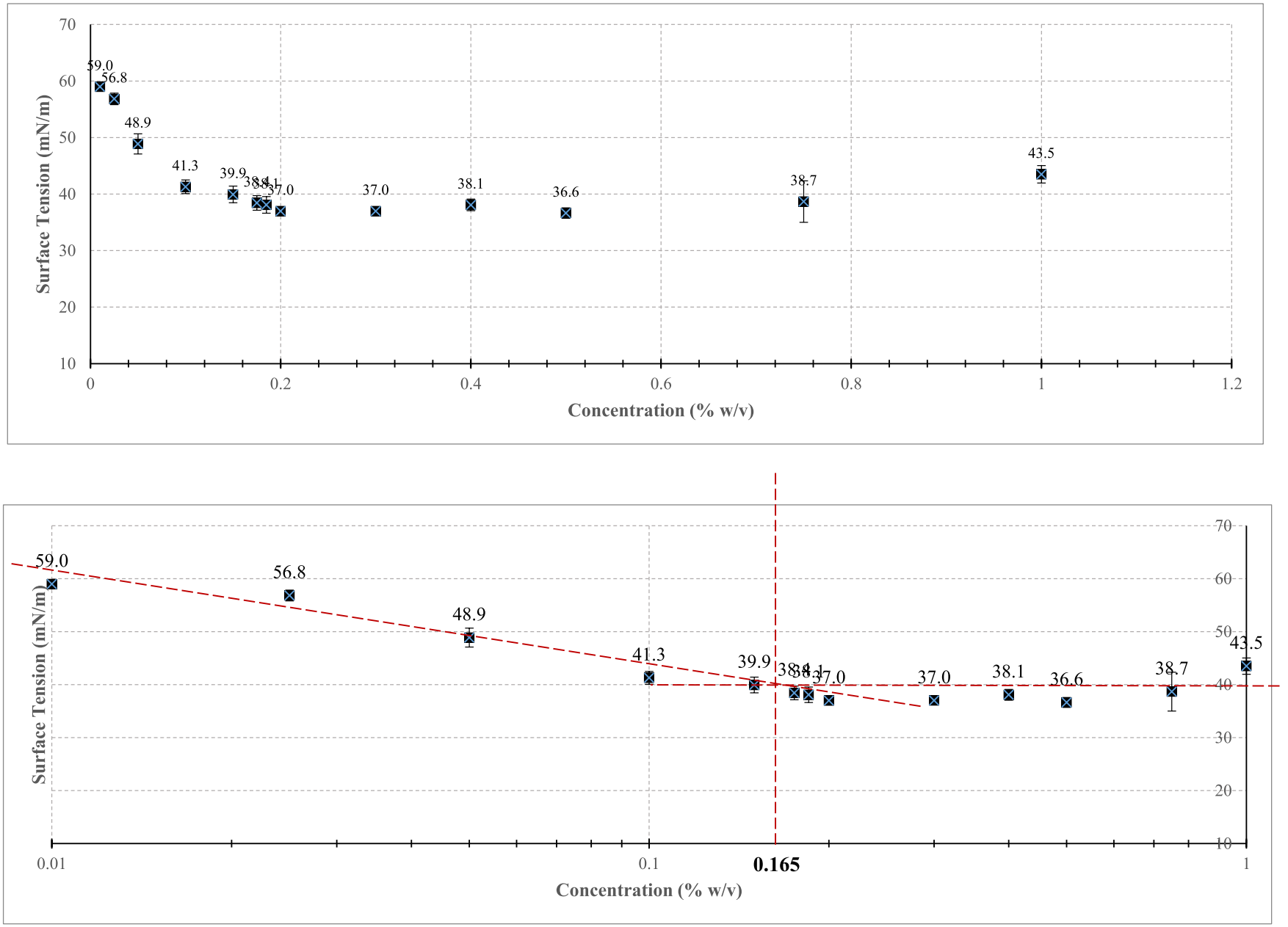

Fig. 2. (a) Equilibrium Surface Tension Isotherm (b) Equilibrium Surface Tension Isotherms (x-axis drawn at a logarithmic scale).

storage modulus ($E^{'}$) and dilatational loss modulus (E'').

$$E = E^{'} + iE'' \tag{3}$$

The real part $E^{'}$ (storage modulus) refers to the recoverable elastic energy stored at the interface after a change in surface area. The imaginary part E'' (loss modulus) refers to the energy dissipated through surface tension relaxation by adsorption of surfactants dissolved in the bulk phase. $E^{'}$ and E'' can be calculated independently from the following equations (Cao et al., 2013);

$$E^{'} = \Delta\gamma \frac{A_0}{\Delta A} cos\theta \tag{4}$$

$$E'' = \Delta\gamma \frac{A_0}{\Delta A} sin\theta \tag{5}$$

where $\Delta\gamma$ is the periodic variation in interfacial stress, ΔA is the periodic variation in interfacial area, and θ is the phase angle between the periodic stress and strain curves.

Interfacial stress and surface area are calculated from the following relations;

$$\gamma = \gamma_0 + \Delta\gamma \sin(\omega t + \theta) \tag{6}$$

$$A = A_0 + \Delta A sin(\omega t) \tag{7}$$

where the parameters γ_0, $\Delta\gamma$, A_0, ΔA and θ are determined by regression using a least-squares method. Once these parameters are found, dilatational storage and loss moduli can be calculated from Eqns. (4) and (5) (E. M. Freer et al., 2003). Readers are advised to refer to a more comprehensive review of oscillatory pendant-drop tensiometry theory (Miller et al., 1996).

2.2.5.2. Dilatational rheology measurements. Dilatational rheology measurements were carried out with the same Ramé-Hart tensiometer (Ramé-Hart Instrument Co., Netcong, NJ, USA) tensiometer used for dynamic surface tension data acquisition. Oscillation in the area was provided by an automated dispenser coupled with a gas-tight syringe, capable of oscillating drop area with a maximum frequency of 0.2 Hz $E^{'}$ and E'' was calculated by fitting area, surface tension, and time data to the above-mentioned equations using DropImage Advanced Software, v.2.2.

Upon preliminary amplitude sweep measurements, a strain of below %10 was found to be suitable to devoid the samples off non-linear effects (data not shown). For 25 μL sized drops, below %1 strain, the moduli could not be calculated due to instrument restrictions. Other researchers have also stated a strain of below %10 to lie within the linear viscoelastic region (Ravera et al., 2010; Rühs et al., 2013). Nevertheless, most disturbances happening during preparation, storage, and transportation of dispersions, cause strains usually higher than this limit. Most interfacial responses in real-life, thus, are non-linear (Mendoza et al., 2014). Eqs. (4) and (5) require the perturbations to be limited to a strain within the linear viscoelastic regime. Consequently, to better represent real-life behavior, strain for oscillation measurements was chosen as %8, which lies within the linear region and is close to that upper limit. Additionally, in order to maintain a Laplacian shape for the oscillating drop, we restrain attention to drops that are not highly viscous (up to 1% w/v QSE).

Similar to the dynamic-tension measurements, surface rheological response is observed over extended time frames. To avoid continually oscillating the same drop for long periods of time, fresh drops are formed for each experiment and aged for 30 min before starting periodic oscillations. The area was varied at a constant strain of 8%, at 10 different frequencies between 0.01 and 0.1 Hz. 40 points were recorded with a period of 4. Experiments were repeated 5 times for each sample. All experiments were performed at 25 °C.

2.2.6. z-average particle size

Quince seed extract mean radius was estimated by calculating z-average particle sizes using a Malvern Zetasizer (Nano ZS, Malvern, UK). The system was based on dynamic light scattering. The method involves the measurement of the self-diffusion coefficient (D, m^2/s) and conversion of it to hydrodynamic diameter (d_H, nm) according to the Stokes-Einstein equation.

$$d_H\left(\times 10^9\right) = \frac{kT}{3\pi\eta D}$$

where k is Boltzmann's constant and T is the absolute temperature (K) (Yang et al., 2012). Experiments were conducted in standard disposable cuvettes at 25 °C with a refractive index of 1.45 for the biopolymer. To ensure observation of aggregate sizes at the pre-determined concentrations, solutions were not diluted. Nevertheless, as confirmed with the software's data quality section, none of the samples displayed multiple scattering. The results obtained are mean of 100 measurements from three replicates each.

2.3. Statistical analysis

Statistical analyses were performed using statistical analysis software (Minitab v16.0, Pennsylvania, USA). For comparison of the means to identify which groups were significantly different from others, analysis of variance (ANOVA) with Tukey's multiple comparison test was used. Differences were considered significant for $p < 0.05$.

3. Results & discussion

3.1. Equilibrium surface tension & z-average particle size

Equilibrium surface tension (ST) measurement is the most accessible and commonly employed surface measurement. It is defined as the capillary force per unit length acting on the interface (mostly reported in mN/m) after the adsorption of the surfactant is finalized (Berg, 2010; Shaw, 1992). Despite its immense popularity in colloidal studies, the measurement of equilibrium surface tension alone provides no information on the dynamic interfacial behavior, which leaves out important interfacial phenomena like rate and mechanism of adsorption, the interface's resistance to shear and dilatational disturbances (Karbaschi et al., 2014). The impact of these complimenting surface processes is established by research that confirms that a reduction in interfacial tension is not the only parameter defining a dispersion's stability. Emulsions of certain paraffin hydrocarbons exhibit poor kinetic stabilities despite displaying considerably low surface tensions. Yet, emulsions stabilized by some large molecular surfactants (such as asphaltenes and resins) show prolonged stability under physical disturbances and even years after their formation (Z. Wang, Zhou, et al., 2014). Nevertheless, equilibrium surface tension is directly proportional to Gibb's free energy of the interface. Any reduction in ST is recognized as a reduction in excess surface energy, which confers dispersions higher thermodynamic stability (Berg, 2010; Z.; Wang, Zhou, et al., 2014). Consequently, using a single value like ST eases the comparison of different surfactants by presenting scientists and the industry with a quantitative indicator of the "performance" of the surfactant on the employed interface.

For large molecular surfactants like quince seed extract, the process of adsorption takes a long time to be finalized. Adsorption process will be examined in more detail in Section 3.2; however, at this point, we believe it is essential to talk about the challenges we came across in the identification of an equilibrium. All samples were subjected to a total of 10 measurements, with 2 of them lasting longer than 12 h (overnight), and the other 8 data were measured for 120 min. Samples continued to relax (especially the ones with concentrations <0.3% w/v) even after 2 h. However, after 2 h ST relaxation process was extremely slow

($\cong 0.5 \frac{mN}{m} per\ hour$). The droplets were measured inside sealed cuvettes, whose inner % RH was preserved close to saturation, which was ensured by filling approximately ¼ of the cuvette with water. The objective of this design was to minimize evaporation and subsequent particle shrinkage. Nevertheless, despite our best efforts, we were not able to completely stop evaporation. The disperser used was automated and was adjusted to keep the particle area constant at all times. Still, we believe, considering the loss in total solution volume in the syringe, evaporation was in place. After a certain amount of time, relaxation processes become so slow that it was not possible to relate the reduction in surface tension with adsorption certainly. ST reduction due to evaporation-induced shrinkage could start to dominate over the adsorption considering the slower rates. For higher concentrations (<0.5% w/v), interestingly, we observed an opposite trend. There was a prolonged increase in ST ($\cong 0.2 \frac{mN}{m} per\ hour$) after the initial decrease. This behavior started after around 1–2 h of droplet formation and was explained by the extract's highly hygroscopic structure. Upon conformational changes during relaxation due to the formation of new free adsorption sites on the air-water surface, some of the water vapor in the cuvette could be attached to the droplet and be adsorbed on the particle surface. This hypothesis was confirmed with marginal increases in syringe volume in overnight measurements. That is why we found it most suitable to report equilibrium ST data as the minimum ST achieved within 120 min of particle formation. Similar challenges were encountered by other researchers as well; some reported that interfacial properties continue to drift even after days of formation for polymeric surfactants (Bantchev & Schwartz, 2003; Beverung et al., 1999; Cascão Pereira et al., 2003; Erik M.; Freer et al., 2004a; Tupy et al., 1998).

Fig. 2a shows the surface tension isotherms that relate the change in quince seed extract concentration with equilibrium surface tension values. QSE, to our surprise, was very influential in displaying a significant reduction in surface tension even in concentrations as low as 0.025% w/v. At 0.025% w/v, QSE reduced ST of water from 72 mN/m down to 58.9 mN/m. Expectedly, higher bulk concentrations also increase the amount of surfactant on the interface, further reducing surface tension. By increasing QSE concentration, it was possible to decrease ST down to around 36.5 mN/m. As analyzed in detail in the previous section, QSE is a large branched polysaccharide that mainly consists of a xylose backbone, with proteins attached to the glucuronic and galactronic acid molecules on the branches and it is these proteins that are primarily responsible for the extract's surface affinity. There are very few biopolymers that naturally contain proteins that have such high accessibility to the surface. Gum Arabic, which is a benchmark emulsifying and stabilizing agent, contains around 1–2% protein, and a concentration of up to 3% w/v of the gum can decrease ST of pure water down to the range of 46–55 mN/m as reported in multiple studies (Bouyer et al., 2013; Cao et al., 2013; X.; Huang et al., 2001). This value is also lower than most other polysaccharide based stabilizers such as guar gum (52.95 mN/m @ 1% w/v concentration), tragacanth gum (47.4 mN/m @ 0.85% w/v) (Moreira et al., 2012), Acacia tortuosa gum (42.6 mN/m @ 0.5% w/v concentration) (Muñoz et al., 2007), Sterculia apetala gum (56 mN/m @ 0.5% w/v) (Pérez-Mosqueda et al., 2013), Acacia Senegal gum (57.4 mN/m @ 0.5% w/v) (Castellani, Guibert, et al., 2010), okra gum (47.9 mN/m @ 0.5% w/v) (Yuan et al., 2019). QSE shows an exceptional reduction in surface tension compared to similar biopolymers. This behavior could be explained by the high hydrophobicity of the gum. As described in Section A.1.4 (See Appendix), the extract's proteins are composed of 37% of hydrophobic amino acids. The hydrophobic portions of the protein also possess high accessibility to the surface, as is apparent in the gum's high surface hydrophobicity.

As demonstrated in Fig. 2a, ST values decrease down to a plateau (~36 mN/m), after which concentration has no effect on ST. This could be explained by the total monolayer coverage of the interface. The concentration where this occurs is reminiscent of critical micellization concentration for small molecular surfactants. Critical micellization concentration (CMC) is defined as the concentration for a specific surfactant-solvent combination at which the surface becomes saturated, and any added surfactant would exist in micelles in bulk (Arabadzhieva et al., 2011; Shaw, 1992). Similar behavior is also witnessed in polymeric surfactants, at which, after a certain polymer concentration (critical aggregation concentration, CAC), further polymer addition produces polymeric aggregates (Krstonošić et al., 2019; Tadros, 2009). Similarly, in our findings, after CAC, QSE addition had no effect on eq. STs. To identify CAC, the most utilized method is to draw linear curves over ST vs. logC curve, and label the point of intersection as CAC (Bu et al., 2004; Dal-Bó et al., 2011; Rub et al., 2013). Fig. 2b, is the ST vs. C curve drawn on a logarithmic scale. The linear trend curves for the decreasing and constant ST sections intersect at a concentration of around 0.165% w/v. This sharp kink point of slope change in ST isotherm curves (Fig. 2a and b) was defined as CAC for QSE at an air-water interface. This means further polymer addition after a concentration of 0.165% w/v does not confer increased thermodynamic stability to an emulsion/foam or help facilitate its initial formation. 0.165% w/v is a relatively low concentration to provide surface saturation. In comparison, Gum Arabic continues to decrease eq ST. up to concentrations of 3% w/v (Cao et al., 2013). Consequently, it is safe to say that QSE can provide similar emulsification properties for much lower concentrations than most similar biopolymers, or ensures much higher stability for the same concentration. The highly hydrophobic nature of the protein and the unique structure of these hydrophobic residues could be the reason for this. It is already well-known for block and graft type copolymers like QSE to have much lower CACs than homopolymers or other copolymers (Tadros, 2009).

Table 2 shows the zeta-sizer measurement results for QSE solutions at various concentrations. Measurement of hydrodynamic radius, determined by dynamic light scattering measurements, is one of the most useful methods for determining polymers' size and conformation. Hydrodynamic radius (R_h) is a measure of the effective size of a polymer and described as the radius of an equivalent hard-sphere diffusing at the same rate as the molecule under observation (Wilkins et al., 1999). The size of a molecule could change depending on external conditions, as is strongly related to the solute-solvent and solute-solute interactions (Tadros, 2011). QSE chain size seems to be around 900 nm when solvated in water (Table 2). However, for concentrations above <0.2% w/v, the polymer sizes suddenly increase to <2500 nm, indicating aggregate formation composed of clusters of several QSE molecules. These polymer aggregates occur due to the close association of hydroxyl groups (abundant in QSE molecule) that have strong hydrogen bonding capacity and are reversible via dilution (Burchard, 2001). The sudden jump in polymer size between concentrations 0.1–0.2% w/v, is in agreement with the CAC identified as 0.165% w/v by eq. ST measurements. QSE aggregates sizes go up to ~3100 nm. Protein aggregates can range in size from nanometers to hundreds of micrometers, yet the size of QSE aggregates is larger than aggregates of commonly employed proteins and protein-polysaccharide combinations. Gelatin-hsian-tsao gum aggregates showed aggregate sizes up to a maximum of 1500 nm (You et al., 2020), major portion of gum Arabic aggregates peaked at around 1000 nm (Isobe et al., 2020), casein micelles peaked around 550

Table 2
z-ave diameters for solutions with different QSE concentrations.

Concentration (% w/v)	*z*-ave (d.nm)
0.05	891 ± 92^a
0.1	989 ± 81^a
0.2	2772.5 ± 251^b
0.3	2287 ± 195^b
0.4	2795 ± 253^b
0.5	3013 ± 193^b
0.6	2619 ± 228^b
0.75	2643 ± 230^b
1	3124 ± 378^b

nm (Chen et al., 2018), soy protein aggregates showed maximum aggregate sizes of 525 nm (Wu et al., 2019), and acid aggregated whey proteins reached a maximum aggregate size of ~2500 nm. QSE's larger molecular weight and highly branched structure could be the reason behind the large aggregate sizes. Molecules with larger sizes, though tend to adsorb more slowly on the interfaces, once adsorbed, form more stable dispersions as a result of the thick gel-like network they form on the interface (Bouyer et al., 2013; Davis & Foegeding, 2006; Erik M.; Freer et al., 2004a).

Equilibrium ST at the highest concentration used (1% w/v) was measured to be higher (at 43.5 ± 0.6 mN/s) than the ST at CAC. An increase in bulk concentration after CAC is expected to have minimal effect on ST. The rise of ST at 1% w/v QSE, could be explained by the viscosity enhancing effect of QSE. Being a bulky polymer, QSE significantly modifies the solution viscosity and changes its flow behavior. Thus, at high polymer concentrations (presumably after a certain critical concentration), the solution viscosity becomes so high that it interferes with the diffusion process, which causes equilibrium to set at a longer time scale. For reason explained previously, long measurements yielded problematic measurements. Hence, equilibrium ST data reported for Q1 might be higher than the actual equilibrium, which is expected to lie around 36 mN/m, same with the ST at CAC. Pérez-Mosqueda et al. (2013) observed similar behavior with S. apetala gum solutions after 1% w/v concentration. They explained this observation with a shift of flow behavior from a Newtonian to a non-Newtonian model at a critical concentration that lies between the two measured concentrations.

The effect of pH and salt content on equilibrium STs are depicted in Fig. 3a and b, respectively. Eq. ST of QSE decreased from 38.5 mN/m to 34.5 mN/m as pH increases from 3 to 11. As stated in Section 1.1, the isoelectric point of QSE is pH 4.2 (Deng et al., 2019). So out of the chosen pHs, pH3 is the one closest to the extract's isoelectric point, where the net surface charge of the gum is zero. QSE is a polyelectrolyte and contains a significant amount of charged groups such as sugar acids and amino acids. These acids are located on the branches, and as we go further away from the isoelectric point of pH 4.2 to basic pHs, more and more of these groups are negatively charged, which increases the overall charge of the molecule up to −38.1 mv at pH10 (Deng et al., 2019). The increased charge at the interface may have promoted electrostatic attraction between polysaccharide and protein molecules, which reduced competition for the interface and yielded more closely packed and thicker, denser interfaces. Higher surface excess concentration is known to result in lower STs. This result seems to be in line with findings of other studies that have demonstrated an increase in QSE's emulsifying and foaming properties as pH moves further away from the isoelectric point (Deng et al., 2019). STs were also significantly affected by the medium's ionic strength, as seen in Fig. 3b. There was no significant difference between eq. STs. of S0.1, S0.3, and S0.5 (lying around ~34.5 mN/m), yet ST without any NaCl for the same concentration was 37.0 mN/m. This means salt addition decreases equilibrium STs. The concentrations used are within the "salting in" range for QSE, as shown by previous studies (Ashraf et al., 2017; Deng et al., 2019; Rezagholi et al., 2019), which means adding more NaCl increases protein solubility. Protein chains are better solvated by water in the presence of Na^+ and Cl^- ions; hence polymer chains spread out more with charged and polar groups extruding through the aqueous phase in well-separated lateral chains. This conformational change eases the unfolding of the proteins, which better exposes the hydrophobic residues to the interface, decreasing surface tension.

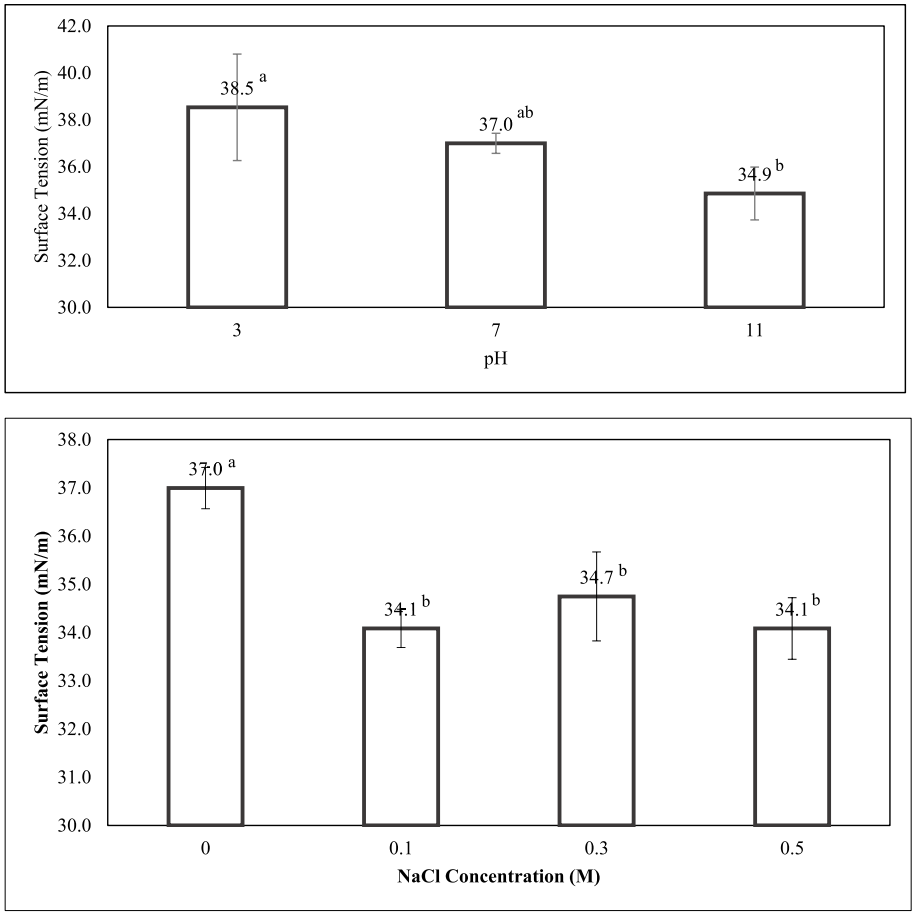

Fig. 3. (a) Equilibrium surface tension of QSE solutions at different pHs (b) Equilibrium surface tension of QSE solutions at different NaCl concentrations.

3.2. Dynamic surface tension curves

For a biopolymer to be an effective foaming/emulsifying agent, in addition to showing surface activity, it should also have the capacity to lower surface tension within the time scales relevant to the emulsification process (P Walstra, 2002; Pieter Walstra & Smulders, 2007). The rate of adsorption as well as the adsorption profile is just as important in assessment of emulsification properties of a surfactant. Especially for polymers, due to their considerable molecular weight, the rate of adsorption is usually slower than small molecular surfactants, and also some processes, such as foaming, requires a rapid positioning on the interface, which further necessitates the investigation of adsorption dynamics (Cao et al., 2013; Erik M.; Freer et al., 2004a; Seta et al., 2014; Wüstneck et al., 1996).

Interfacial adsorption of surface-active materials is governed by surface pressure changes with an adsorbent concentration on the surface. According to *Le-Chatelier* principle, the direction of equilibrium would shift in the direction which stress can be relieved. For surface active biopolymers dissolved in solution bulk, interactions between polysaccharides and the interface is more favorable that of solvent and the interface (Wüstneck et al., 1996). Consequently, adsorption occurs spontaneously and causes increasing surface pressure up to an equilibrium value. There are well-established adsorption theories for low-molecular-weight surfactants, yet in the case of polymers, no such model exists (Kontogiorgos, 2019b; Wüstneck et al., 1996). Langmuir isotherm, however, is demonstrated to be a close approximation to the real protein adsorption process and was used for estimation of the diffusion coefficient in surface studies (Santini et al., 2007; Tadros, 2009; Wüstneck et al., 1996).

The dynamic ST vs concentration curves can be seen in Fig. 4. For ease of comparison, only the first 30 min were shown on the graph. As previously discussed, the data reliability decreases for longer times. As the relaxation rate decreases, other processes such as evaporation of adsorption of water become more dominant, making the curves harder to interpret. As seen in Fig. 4, the adsorption curves for the first 30 min seems to consists of two regions with distinctly different slopes, with an initially high relaxation rate that significantly decreases after around the 200–400 s mark. This kink in slope refers to a change in the mechanism of ST relaxation. Only one of the samples (Q0.01) follows a different relaxation profile that contains an additional lag phase where ST does not drop within the initial 200 s. This behavior is reminiscent of typical protein adsorption that occurs in three different regimes. A representative curve is given in Fig. 5. The first of these, Regime I, is only observed for dilute concentrations. During this period, because of the possible existence of kinetic barriers to surfactant adsorption over the measured time scale, there occurs no drop in ST (Adamczyk et al., 2009; Beverung et al., 1999; Macleod & Radke, 1994; Pérez-Mosqueda et al., 2013). This regime, also called induction or lag period. This phenomenon is interpreted in several ways. Such a mechanism proposes a phase transition related to intermolecular attraction supplemented by diffusion and adsorption of additional surfactant molecules that do not create changes in surface tension. Another such mechanism explains this behavior, co-operative adsorption caused by intermolecular attractions, which causes the activation energy for desorption to increase faster than adsorption. The presence of interaction due to co-operative adsorption reduces surface pressure which compensates for the ST reduction owing to the increase in surface concentration (Calero et al., 2010). In any case, due to the slow rate of diffusion, or interfacial unfolding and rearrangement of globular proteins, STs do not drop appreciably during this period (Beverung et al., 1999; Nahringbauer, 1995; Pérez-Mosqueda et al., 2013).

We have only observed an induction period for a concentration of

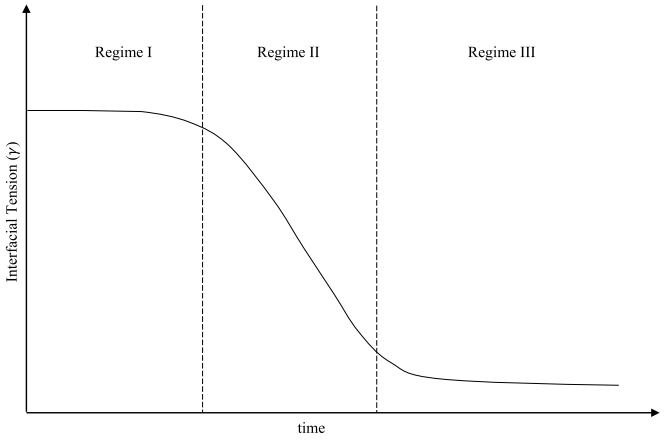

Fig. 5. A representative curve displaying typical dynamic interfacial tension response of polymeric surfactants in dilute solutions.

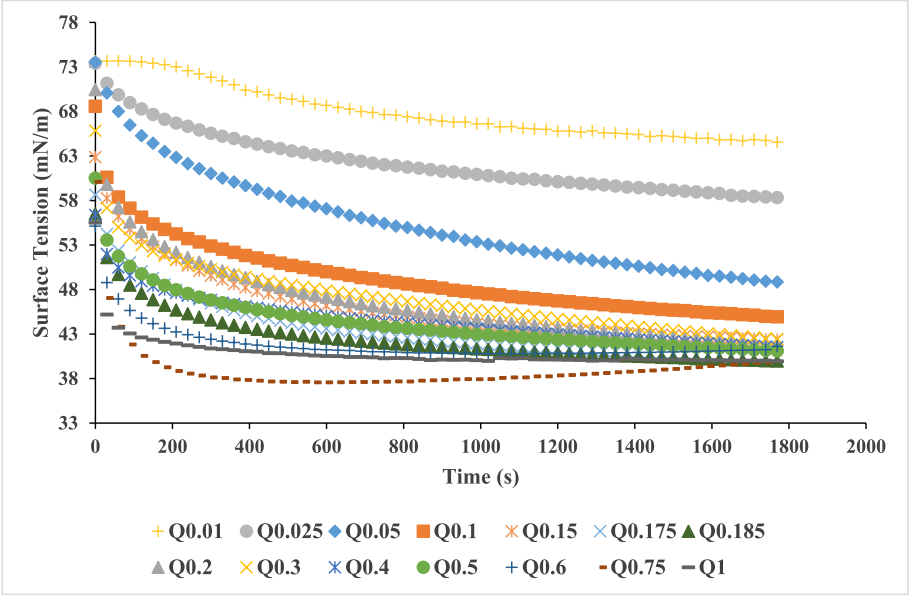

Fig. 4. Effect of concentration on the surface tension profile of QSE solutions.

0.01%, at which the equilibrium ST was around 63 mN/m. Due to the scarcity of QSE in bulk at such low concentrations, the effective diffusion coefficient, which is a function of concentration, is so small that a period of constant ST is observed. For concentrations larger than 0.025% w/v, the relaxation curves proceed to Regime II so quickly that it cannot be observed within the time scale of the pendant drop method. For foams, a rapid interfacial acquisition is necessary. Molecules that do not require an unfolding to show interfacial activity have been demonstrated to be better suited for foam formation. These molecules that can directly adsorb on the interface in their native state have shown no induction period, and this attribute was reported to contribute to their foamability (Davis & Foegeding, 2006; Zhu & Damodaran, 1994). With rapid adsorption, the interface acquires higher resistance against disturbances in the form of energy input introduced during foam formation, which hinders foam collapse. Due to differences in surface affinity and denaturation kinetics, different polymers display vastly different relaxation profiles (Beverung et al., 1999). The fact that QSE does not display an induction period for concentrations over 0.025% w/v designates its strong potential as a foaming agent.

For concentrations over 0.025% w/v, relaxation of ST starts within the first few seconds of particle formation. A higher concentration of the surfactant polymer in bulk results in an almost instant acquisition of an interfacial concentration above the critical value necessary to observe ST reduction. The next relaxation phase (Regime II in Fig. 5) is identified with a sudden decline in ST and for all QSE concentrations it was over within the first 200 s. During this phase, molecules diffused to the interface partially expose hydrophobic residues to the air-water surface and are irreversibly adsorbed (Macritchie, 1978; Vrij, 1976). The steep decline in surface tension is explained by two mechanisms that act simultaneously. Adsorbed molecules relax from their rigid conformation that makes room for more of the hydrophobic sections of the molecule to be adsorbed, increasing the number of contacts for each molecule. At the same time, new molecules continue to diffuse from the bulk aqueous phase and be adsorbed, either in their native state or with minimal conformational change. This process continues until interfacial saturation (Beverung et al., 1999).

The lack of an induction period and the very steep ST decline is a rare observation in surfactant biopolymers. For globular proteins, for instance, a lag period is commonly observed, and Regime II ST reduction progresses at a slower rate (Beverung et al., 1999; Covis et al., 2014; Dickinson, 2018; Karbaschi et al., 2014; Sosa-Herrera et al., 2016). This finding implies that QSE proteins, even in their native state, and the polysaccharide chains solvated in water, contain hydrophobic residues with instant access to an interface. The high surface hydrophobicity of QSE implies that the tertiary structure of the proteins is aligned such that the hydrophobic amino acids are not embedded into the molecule interior. Protein surface hydrophobicity was found to be directly related to the rate of tension decline in Regime II by Beverung et al. (1999), who have shown casein and BSA that displays the greatest rates of ST decline to also possess the highest surface hydrophobicities out of the proteins investigated. As summarized in Section A.1.3 in Appendix, QSE is composed of three different polysaccharide-protein complexes, with some of them being smaller than others. The smaller glycoproteins could have rapidly diffused to the interface and started ST decline, which could have been supported by subsequent irreversible adsorption of the much larger QSG2. A similar observation was made for Gum Arabic. The consensus is that the AGP (arabinogalactan-protein) component is the fraction primarily responsible for Gum Arabic's interfacial properties, with the glycoprotein fraction taking a supplementary role (Evans et al., 2013; Funami et al., 2007; Kontogiorgos, 2019b; Sanchez et al., 2018). It is known that with polydisperse polymers, the more significant molecular weight fractions adsorb preferentially over smaller ones and with time, especially at higher concentrations, they replace smaller fractions that are much quicker to be positioned on the interface (Cao et al., 2013; Tadros, 2009). The rate of relaxation in Regime II, expectedly, increases with increasing concentration. With higher concentration of surfactant in bulk, the molecules' accessibility to the surface increases. The rate of diffusion also increases owing to the shortened mean free path for diffusion. A more crowded solution also increases the rate and probability of molecular collisions, increasing interfacial positioning of the protein molecules (Young & Torres, 1989). Many other researchers have also reported increasing relaxation rate with surfactant concentration (Arabadzhieva et al., 2011; Bouyer et al., 2013; Moreira et al., 2012; Pérez-Mosqueda et al., 2013; Sosa-Herrera et al., 2016; W.; Wang, Zhou, et al., 2014; Young & Torres, 1989).

The final regime starts around the 200 s mark and continues until the end of time-dependent measurements. As previously discussed, QSE at the air-water interface never displayed a proper equilibrium. The slower gradual decline in Regime III (Fig. 5) is associated with conformational changes in the adsorbed layer and the resulting interfacial skin formation (Benjamins & van Voorst Vader, 1992; Cascão Pereira et al., 2003). With ongoing slow rearrangements, adsorbed molecules tend to seek the most energetically favorable positions for their hydrophobic and hydrophilic side chains. During this process, more and more of the hydrophobic sections are exposed to the interface, whereas the rest of the molecule, through increased intermolecular attractions, form aggregates, branches, and protein-polysaccharide complexes (Erik M. Freer et al., 2004a; Krstonošić et al., 2019; Sosa-Herrera et al., 2016). The enhanced degree of entanglements form bridges that connect at various points, resulting in an amorphous gel-like network at the interface (Beverung et al., 1999; Erik M. Freer et al., 2004a). For surfactant polymers, this stage goes on for such a long time at a slow rate, making it hard to distinguish a true equilibrium ST. Multilayer adsorption, long-time molecular rearrangements, breakage, and generation of non-covalent stabilizing bonds and interactions between adjacent proteins in solution bulk continue to contribute to ST changes, sometimes over a period of days (Ward & Tordai, 1946; Wüstneck et al., 1996). The slope of ST decline in Regime III, decreases with increasing concentration (Fig. 4). This was quite the opposite of our observation with the relaxation in Regime II. The relaxation rate in Regime II had increased with increasing concentration. After the critical aggregation concentration of 0.165% w/v, all samples equilibrated at the same ST plateau (38 mN/m). However, as the QSE concentrations increased, it took longer to reach that equilibrium. This behavior may be related to the restriction of molecular mobilities by enhanced viscosity of the solution. As previously examined by the authors, QSE causes significant increases in viscosity and a shift from Newtonian to a non-Newtonian flow behavior over a concentration of 0.05% w/v (Kirtil & Oztop, 2016).

The electrostatic effect also plays a significant role in the conformation of the adsorbed layer. The relative contribution of these electrostatic effects is obviously dependent on the pH and the ionic strength of the aqueous medium. Fig. 6a shows the dynamic ST relaxation curves for solutions at different pHs. There is an obvious increasing trend in the relaxation rate as the pH increases from 3 to 11. The isoelectric point of the proteins of the extract is pH 4.2 (Deng et al., 2019). Thus, out of the pHs examined, pH3 is the one closest to the isoelectric point, thus moving to higher pHs, we get further from the isoelectric point. QSE has a high charge density, owing to an abundance of glucuronic and galacturonic acid residues as well as the high protein content. At pH10, the zeta potential of the extract is −38.4 mV. Over a pH of 4.2, proteins are negatively charged; this is also higher than the pKa's of both galacturonic (pKa of 3.5) (Dickinson, 2018) and glucuronic acid (pKa of 3.12) (H. M. Wang et al., 1991). At pH values close to 4.0, uncharged polymer chains readily self-associate. Due to a lack of electrostatic repulsion, molecules tend to locate in close proximity where hydrophobic interactions become dominant. This causes a thinner and denser adsorbed layer with decreased interactions with the aqueous phase. For this case, the free volume associated with each chain is lower, and the reduced conformational entropy restricts the addition of new polymer chains on the interface. The dense packing also makes it harder for the already adsorbed chains to relocate and increases the time it takes for the molecules to relax to their most energetically favorable state (Alba et al.,

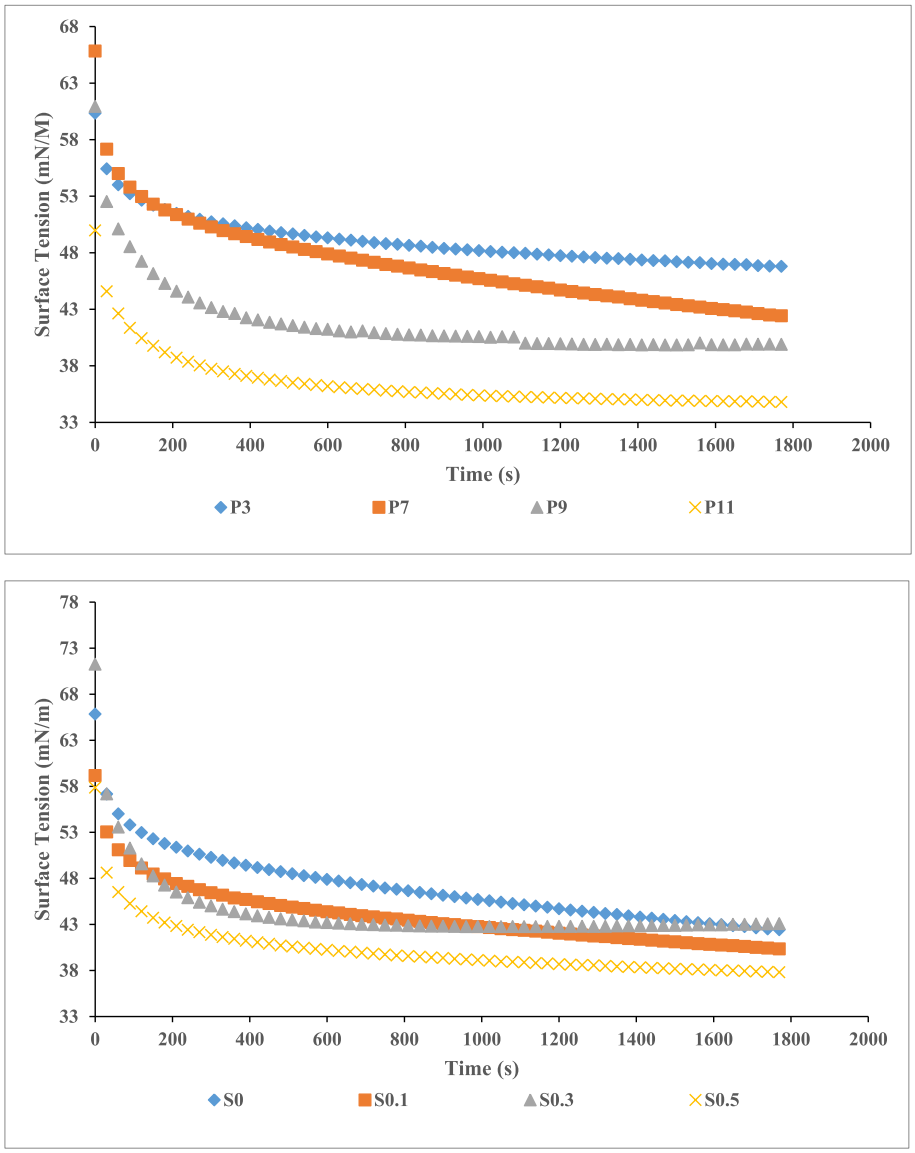

Fig. 6. (a) Effect of pH on the surface tension profile of QSE solutions (b) Effect of NaCl concentration on the surface tension profile of QSE solutions.

2016; Castellani, Al-Assaf et al., 2010). This hindering effect of pH in protein unfolding and the resulting diminished surface activity was also encountered by Deng et al., 2019, who have discovered QSE to show the lowest emulsifying ability index (EAI), emulsion stability index (ESI), and foaming capacity for pHs near 4.0 (Deng et al., 2019).

For pH values well above 4.2, electrostatic repulsion between the negatively charged carboxylic acid groups and the proteins cause the polymer chains to extend further from the interface, increasing water-QSE interactions, which is also supported by increased protein solubility at higher pHs (Deng et al., 2019). As a result, hydrophilic molecule fractions extrude through the bulk phase in a more wide-spread manner, providing more room for fresh molecules to be adsorbed. Additionally, the reduced hydrophobic interactions within the molecule itself result in accelerated structural flexibility that increases molecular mobility, facilitating molecular rearrangements. All these increase the rate of relaxation of the polymer for pHs higher than 4.2. At pH11, the equilibrium ST is also significantly lower than other pHs by around 2 mN/m. This implies that, with the increased negative charge, after a certain point, not only the rate of unfolding, also the final state of the molecule changes. QSE is abundant in disulfide bonds (19.79 μM/g as identified by method), which is known to provide high structural stability of proteins and can act as a barrier against protein denaturation (Beverung et al., 1999; Du et al., 2012; Karbaschi et al., 2014; Tang et al., 2006). The high charge at pH11 presumably was sufficient to break the final remaining disulfide bonds and overcome other possible intermolecular attractions that prevent complete unfolding. As a result, the final remaining hydrophobic residues are exposed to the air-water interface resulting in a decline in ST. Other researchers have similarly observed increased surface activity of proteins further from the isoelectric point (Mundi & Aluko, 2012; Tang et al., 2006).

Fig. 6b shows the ST relaxation profiles of QSE solution with differing amounts of NaCl (S0: control, S0.1: 0.1 M, S0.3: 0.3 M, S0.5:

0.5 M). Addition of a background electrolyte species (e.g. NaCl) to a polyelectrolyte solution results in the formation of an ionic double layer. All these ions are only soluble in the aqueous phase and simultaneous transport of each species is finalized when surface-active ions (e.g. QSE anions), are completely covered by its associated indifferent counter-ion (e.g. sodium cations) which is surrounded by an indifferent co-ion (e.g. chloride anions). Ions within the double layer are anchored to their positions surrounding the interface by a series of electrostatic attractions and repulsions (Gao et al., 2017; Macleod & Radke, 1994). This could later act as a shield against the transport of nonionic surfactants in particular. For charged polymers, the salt screening effect can facilitate adsorption (Young & Torres, 1989). For our case, the presence of an ionic double layer enhanced the rate of transport of surfactant and its adsorption. A higher ionic strength solvent is known to reduce the Debye length of charged protein side chains (Beverung et al., 1999a). As a result, electrostatic repulsion decreases, allowing for faster interfacial saturation and helps the proteins to pack in a more efficient way. Similarly, the charged sugar acids that are not adsorbed but extrude through the aqueous phase, being negatively charged at neutral pH, can form a layer of charge-charge repulsion that acts against the movement of surfactants towards the interface. The accumulation of Na + cations around the surfactant-laden interface decreases electrostatic repulsion and accelerates the adsorption of fresh polymers. Similar findings were reported by other researchers studying the effect of ionic strength on surface properties of charged surfactants (Beverung et al., 1999b; Hayase & Tsubota, 1986; Ishimuro & Ueberreiter, 1980; Young & Torres, 1989).

3.3. Surface rheology measurements

Despite surface affinity being necessary for forming a dispersed system with a large interfacial area, actual long-term stability is enabled through improved resistance of interfaces from surrounding dispersing phases (Bos & Van Vliet, 2001; Dickinson, 1998, 1999, 2001). Especially for systems stabilized by macromolecular surface-active species, this resistance is more pronounced. The gel-like network formed by adsorbed thick polymer layer results in generating an elastic interfacial skin (Erik M. Freer et al., 2004b) that acts as a barrier against droplet coalescence (Santini et al., 2007). However, a simple visual analysis doesn't provide much quantitative information on the interfacial skin's mechanical properties, formation kinetics, and relaxation rates. This ambiguity is overcome by interfacial rheological measurements that convey information on the interface's response to both the compressional and shear deformation (Langevin, 2000). A highly stable interface should be able to dampen external disturbances both normal and tangential to the interface; that way, film rupture can be prevented. Unlike surface tension, which measures forces normal to the interface, dilatational surface rheology is related to forces operating tangentially, which further underlines its significance (Santini et al., 2007). The theory is also supported by experimental data that shows a direct relationship between surface dilatational properties with foam and emulsion stability (Beverung et al., 1999; Cao et al., 2013; Cascão Pereira et al., 2001; Davis & Foegeding, 2006; Erik M.; Freer et al., 2004a; Kontogiorgos, 2019c; Mendoza et al., 2014; Pérez-Mosqueda et al., 2013; Santini et al., 2007; Vernon-Carter et al., 2008; Zhang et al., 2011).

Table 3
Average E', E'' and tanΔ values.

Concentration (% w/v)	E' (mN/m)	E'' (mN/m)	tanΔ
0.05	58.18 ± 9.41	8.71 ± 2.07	0.15 ± 0.01
0.1	48.5 ± 2.09	9.55 ± 0.26	0.20 ± 0.01
0.2	46.52 ± 1.74	13.12 ± 3.17	0.29 ± 0.07
0.3	47.99 ± 1.54	13.42 ± 1.61	0.29 ± 0.03
0.4	42.85 ± 5.02	11.83 ± 1.96	0.28 ± 0.02
0.5	45.72 ± 3.75	13.98 ± 2.34	0.32 ± 0.03
0.6	24.63 ± 4.63	7.41 ± 0.87	0.31 ± 0.02
0.75	22.35 ± 7.88	7.08 ± 2.26	0.33 ± 0.04
1	23.48 ± 1.91	7.89 ± 1.01	0.34 ± 0.04
pH			
3	40.77 ± 1.97	7.23 ± 0.29	0.18 ± 0.01
7	47.99 ± 1.54	13.42 ± 1.61	0.29 ± 0.03
11	29.79 ± 8.08	9.44 ± 1.96	0.36 ± 0.11
Salt Content (M)			
0	47.99 ± 1.54	13.42 ± 1.61	0.29 ± 0.03
0.1	37.80 ± 1.77	11.11 ± 1.61	0.30 ± 0.03
0.3	28.68 ± 7.00	7.29 ± 1.88	0.26 ± 0.01
0.5	41.21 ± 0.68	10.26 ± 1.31	0.26 ± 0.03

Table 3 lists the average values for E' and E'' of 10 different frequencies (from 0.01 to 0.1 Hz). E' (dilatational storage modulus) is a measure of the elastic counterforce of the surface to a possible deformation, whereas E'' (dilatational loss modulus) defines how fast the initial values of ST is restored after deformation (Mendoza et al., 2014; Seta et al., 2014). For all concentrations, elastic behavior is more prominent on the air-water interface. This implies that the viscoelastic interface formed by QSE adsorption behaves more like an elastic solid than a viscous fluid, which bestows the surface a higher resistance to deformation. This behavior is typical for viscoelastic polymer layers (Pérez-Mosqueda et al., 2013). Perfectly elastic interfaces store all of the energy input by deformation, later to release it without loss. Consequently, with higher elasticity, the interface gains a higher resistance against deformation (Erik M. Freer et al., 2004a). A film subjected to stretching by external disturbances increases in surface area, which results in a reduction in surface excess concentration of the foaming agent (called *Gibbs* effect). If enough time passes for surfactants soluble in the bulk phase to diffuse to the surface, original ST can be restored (*Marangoni* effect). The *Gibbs-Marangoni* effect is necessary for foam formation, and the absence of this mechanism is why pure liquids do not foam (Shaw, 1992).

For foams, one of the most dominant destabilization mechanisms is film rupture. The process always proceeds by local thinning on the fluid surface formed by a greater expansion of the surface area in a certain region of the interface. This leads to a dilution of surfactant on the thinning region and results in a surface tension gradient (Karbaschi et al., 2014; Santini et al., 2007). It takes time for the surfactant to be transported from the rest of the interface and the bulk to the thinning region. During this time, the thinning region is considerably more susceptible to rupture than the rest of the interface. Surfactant diffuses to this region, carrying a significant amount of underlying solution, which nullifies the thinning process. The interface requires a high *Gibbs* elasticity to counter the effects of local thinning during the surfactant transport process. Nevertheless, a highly viscous surface (identified by a higher dilatational loss modulus) acts opposingly to this mechanism. High bulk viscosity is expected to retard the rate of foam collapse; on the contrary, high surface viscosity can strongly inhibit bulk fluid and surfactant transport at and close to surfaces, which causes more rapid film drainage (Arabadzhieva et al., 2011; Shaw, 1992). Thus, a highly elastic and less viscous surface provides the highest possible stability against foam collapse. This underlines the importance of phase angle (*tanΔ*), which depicts the ratio of the loss to storage modulus. Hence, the lower *tanΔ* the more stable a foam formed by this surfactant will be. The fact that *tanΔ* values are below 0.36 for all samples, suggests that the interface exhibits a higher elastic character, which implies that QSE would be a potentially effective foaming agent.

Fig. 7 shows the frequency dependence of all E' and E'' of all samples. Surface elasticity (ε_r) and surface viscosity (η) is are a function of both bulk surfactant concentration (c) and frequency (ν). The extend of these dependencies are also known according to the equations of $\varepsilon_r(\nu, c)$ and $\eta(\nu, c)$ identified by van den Tempel and Lucassen (Lucassen & Van Den Tempel, 1972a; 1972b). Studying frequency dependence is crucial as it provides information on the relative importance of relaxation processes like diffusion-adsorption and/or molecular rearrangements (Santini et al., 2007). E' and E'' of all QSE solutions displayed very similar trends

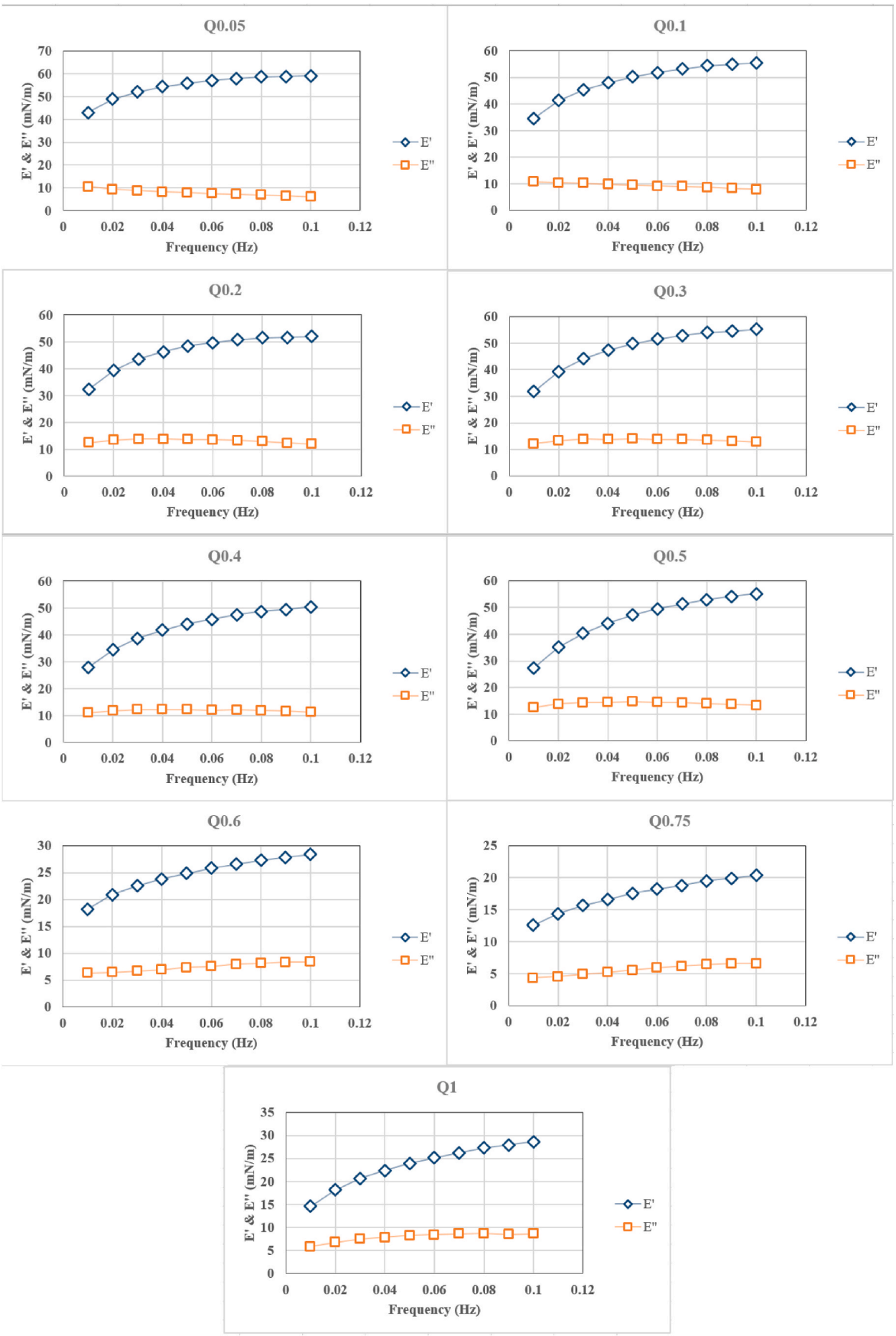

Fig. 7. (a) Frequency dependence of E' and E'' of QSE solutions with varying concentrations (b) Frequency dependence of E' and E'' of QSE solutions with varying pHs and NaCl concentrations.

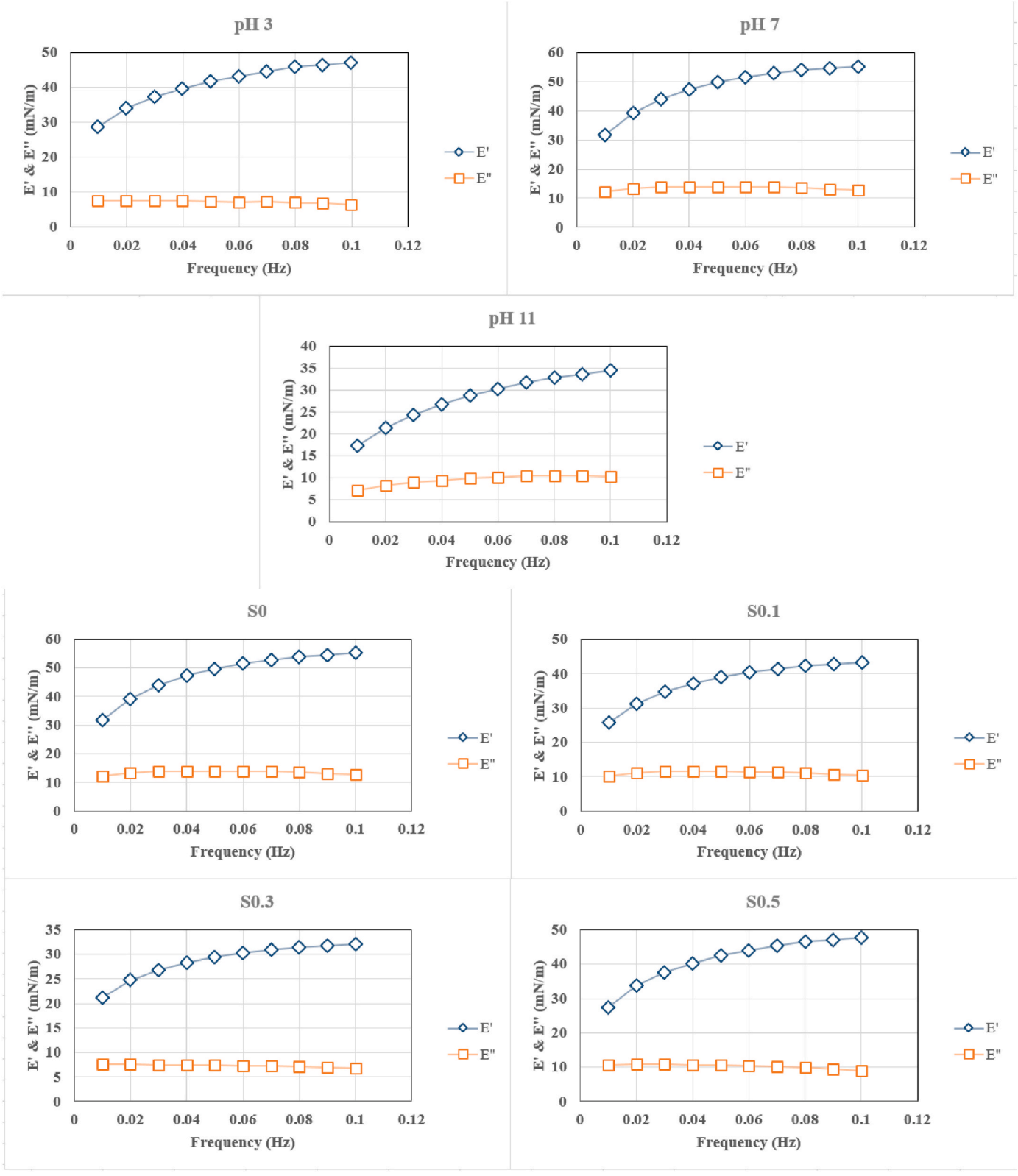

Fig. 7. (*continued*).

with frequency. E' was higher than E'' for all frequencies. E' for all concentrations, pHs and ionic strength, displayed an increasing trend with increasing frequency. E'', on the other hand, stayed constant within the frequency range studied (0.01–0.1 Hz). The increase in E' with frequency is non-linear, with an initially higher dependence on frequency that seems to decrease for frequencies over 0.04 Hz.

As the surface monolayer is directly in contact with a bulk surfactant solution, the surface rheological properties are strongly influenced by adsorption and desorption processes. Expanding (compressing) the monolayer causes adsorption (desorption) of the polymeric surfactants to diffuse from (to) the bulk phase in order to re-achieve its equilibrium state (Cao et al., 2013; Santini et al., 2007). Real behavior lies within two extreme cases. When surface deformation is slow (low frequencies), the monolayer has enough time to reach equilibrium, so much so that deformation has almost no effect on ST. For this case, there is no resistance to expansion ($\varepsilon \rightarrow 0$). When the deformation is so rapid (high frequencies) that the monolayer has no time to respond, it behaves like an insoluble layer, and a change in surface area is directly observed as a similar change in ST (perfectly elastic case). The frequency range obviously lies within these two extremities. According to this mechanism, it is expected for E' to increase with increasing rate of area deformation until a certain plateau is reached (Cao et al., 2013; Ma et al., 2011; Ravera et al., 2005; Z. L.; Wang et al., 2011). The reason for the change in slope with increasing frequency shows E' approaching the plateau value. The initial high dependency of E' on ν, suggest that effect of diffusion of molecules between the bulk and interface on dilatational rheological properties of the surfactant monolayer is more dominant for low frequencies ($\leq 0.4\ Hz$).

E'' staying constant within the frequency range studied indicates that the characteristic frequency of the relaxation process at the surface layer is higher than the highest oscillating frequency used in measurements (0.1 Hz) (Cao et al., 2013; Ma et al., 2011; Ravera et al., 2005; Z. L.; Wang et al., 2011). The frequency range chosen was restricted by the instrument's limitations. This means that rapid relaxation processes dominate surface relaxation, those with characteristic frequencies higher than 0.1 Hz. Since QSE molecules are very bulky, molecular rearrangements would occur at lower frequencies, as observed by Cao

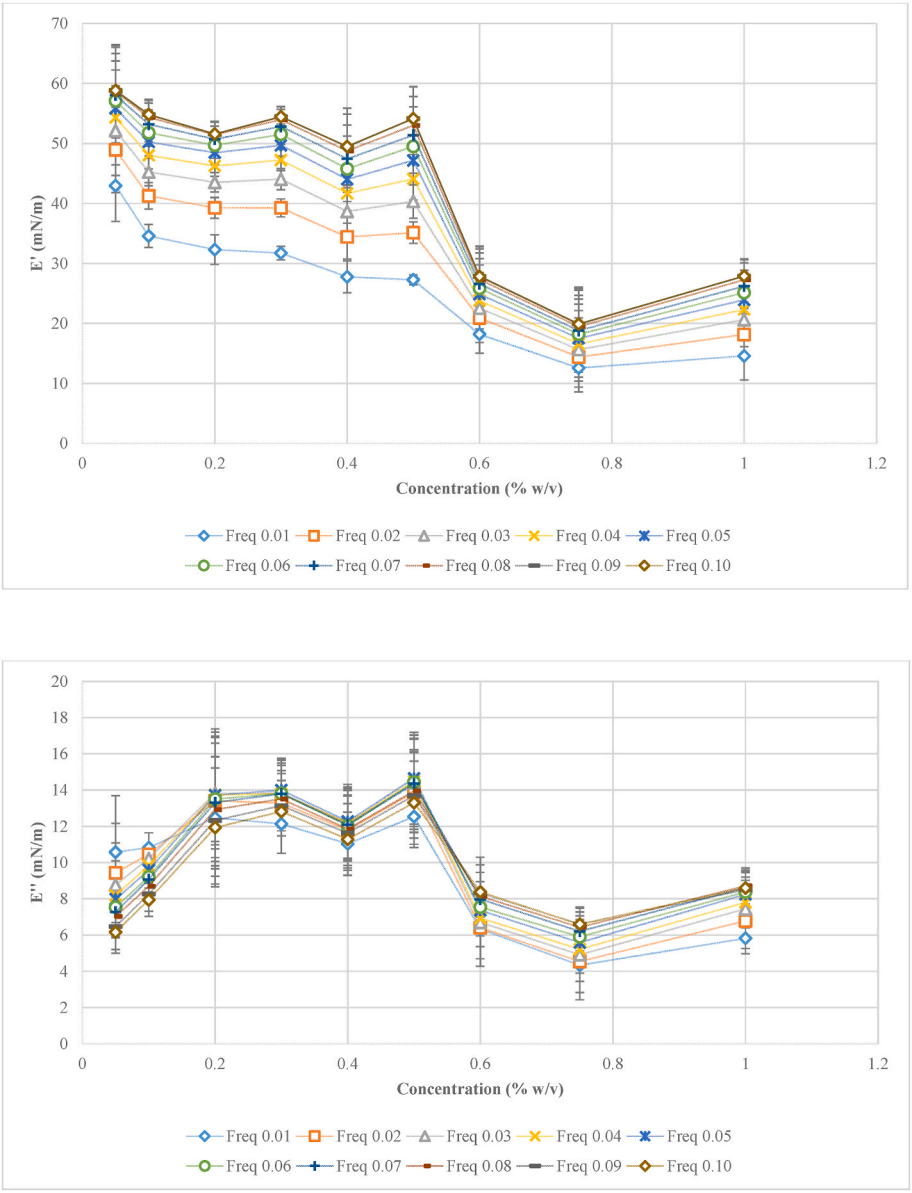

Fig. 8. Concentration dependence of (a) E' (storage modulus) (b) E'' (loss modulus), pH dependence of (c) E' (storage modulus) (d) E'' (loss modulus), NaCl concentration dependence of (e) E' (storage modulus) (f) E'' (loss modulus) for frequencies 0.01–0.1 Hz.

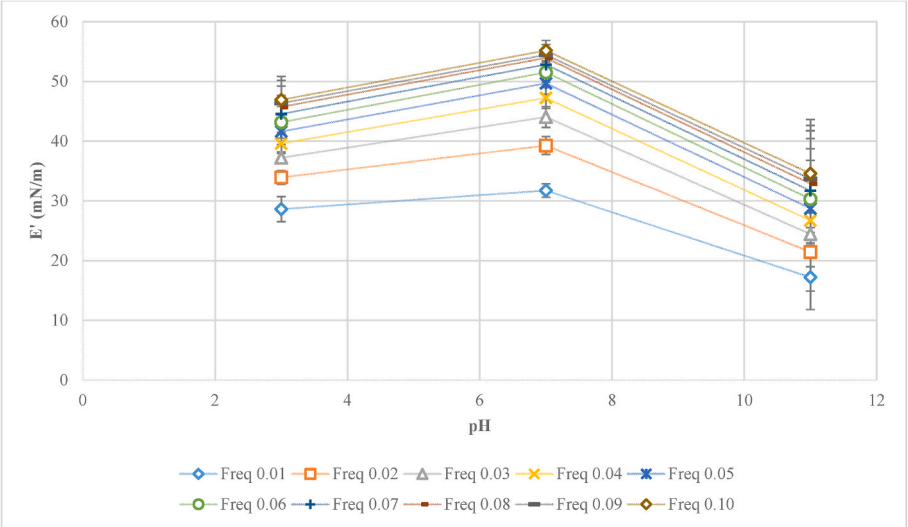

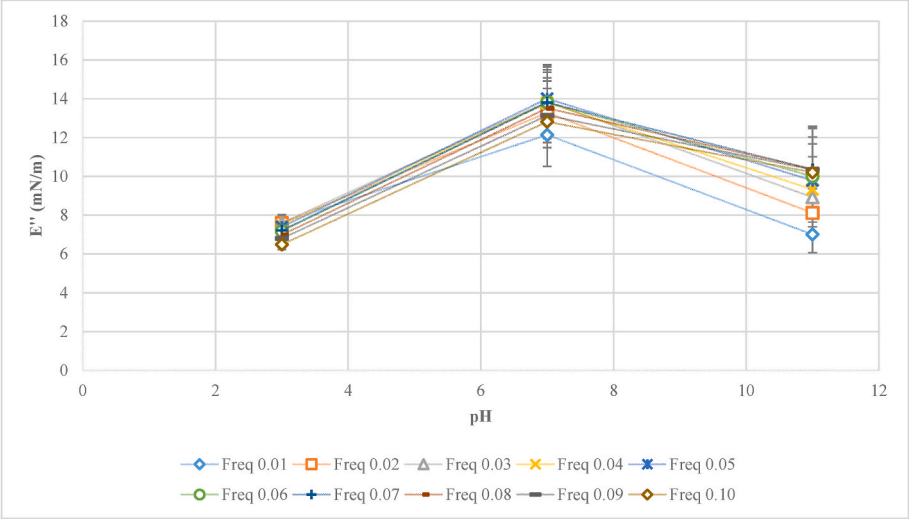

Fig. 8. (*continued*).

et al. on silwet408, a surfactant with a much smaller molecular weight than QSE (Cao et al., 2013). If the effect of molecular rearrangements were dominant, the opposing effects of diffusion and surface repositioning would presumably cause a local maximum within the frequency range studied (Pérez-Mosqueda et al., 2013; Rühs et al., 2013). Consequently, it is safe to say diffusion of fresh surfactant molecules to void sites on the interface is the primary mechanism of relaxation for frequencies between 0.01 and 0.1 Hz.

Fig. 8 shows the concentration, pH, and ionic strength dependence of surface dilatational rheological properties of QSE. With concentration, all frequencies follow a similar trend. The results are the average of at least eight different measurements. Despite the strange zig-zag behavior, the fact that all frequencies follow the same trend implies that the behavior should result from a conflict between opposing mechanisms, one of which becomes more dominant for concentrations over 0.5 w/v. The effect of bulk surfactant concentration on dilatational modulus was explained by *van den Tempel and Lucassen* model (Ma et al., 2011). One of the mechanisms is related to the molecular interactions between the surface and adjacent bulk phase; the other is related to the surfactant concentration on the surface. With an increase in concentration, more and more molecules are available to the interface, resulting in a thicker interfacial network with stronger intermolecular interactions. The thick polymer layer is associated with a higher dilatational modulus and dilatational elasticity. However, on the other hand, higher bulk concentration causes increased molecular exchange between bulk and the interface, which decreases the interfacial tension gradients and thus, results in a reduction in dilatational modulus and elasticity. As a result, as the interface becomes saturated with polymer, the elasticity-enhancing effect of a thicker polymer layer is compensated and finally dominated by the decreased elasticity related to an increased molecular exchange. For this reason, it is to be expected to observe several maxima up until a concentration where one of the mechanisms prominently dominates. Multiple other researchers have similarly reported the presence of one or a few maxima and the company of a sharp kink in slope E' vs c curves (Arabadzhieva et al., 2011; Cao et al., 2013; Rühs et al., 2013; Santini et al., 2007; W. Wang, Zhou, et al., 2014). As

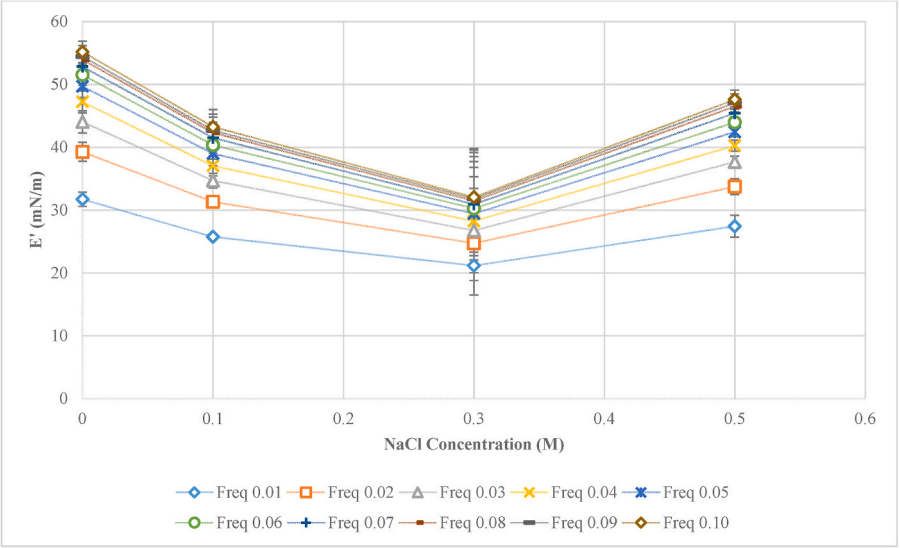

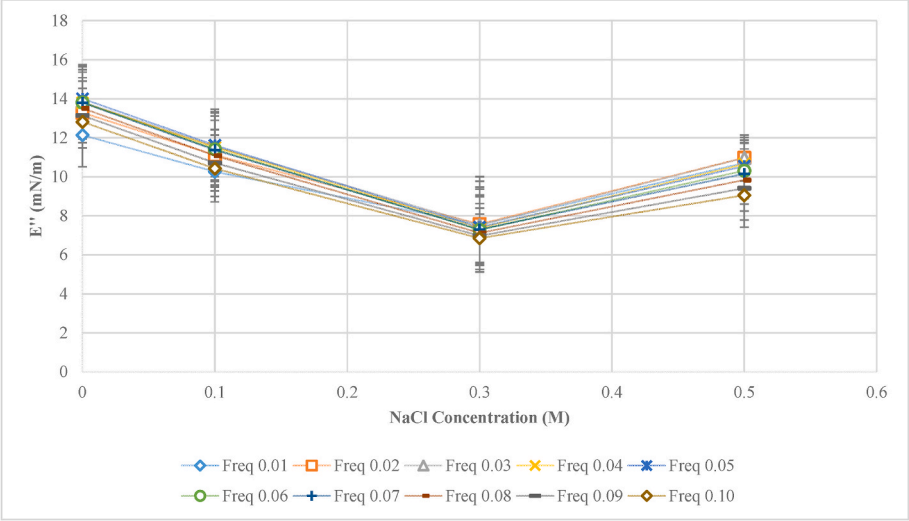

Fig. 8. (*continued*).

depicted in Fig. 8a, the dominance of molecular exchange occurs at a concentration of 0.5% w/v, after which surface dilatational storage modulus decreases significantly (less than half of its initial value). As previously discussed, there is a strong relation between foam stability and E' values, demonstrated in a number of studies (Beverung et al., 1999; Cao et al., 2013; Cascão Pereira et al., 2001; Davis & Foegeding, 2006; Erik M.; Freer et al., 2004a; Kontogiorgos, 2019c; Mendoza et al., 2014; Pérez-Mosqueda et al., 2013; Santini et al., 2007; Vernon-Carter et al., 2008; Zhang et al., 2011). Consequently, a concentration of 0.5% w/v is the highest bulk concentration for a QSE stabilized dispersion, where the interface possesses the highest stability against deformation and the resulting foam collapse or coalescence.

There also seems to be a frequency-dependent shift in local maximum at E' vs c curve (Fig. 8a). Maximum is shifted to higher concentrations with increasing frequency. For frequencies over 0.04 Hz, the maximum concentration that displays the highest loss modulus is 0.05% w/v. For lower frequencies, loss modulus starts following a linearly decreasing trend, with the slope increasing as the frequencies go lower. When discussing surface rheological properties, as previously mentioned, two different frequencies need to be considered, namely, the frequency of molecular exchange (μ) and the disturbance frequency (ν). If the frequency of molecular exchange does not lie within the disturbance frequencies applied (0.01–0.1 Hz), it is impossible to see a maximum. The maximum modulus value is actually the cross-over point where the change from $\mu < \nu$ to $\mu > \nu$ takes place (Stubenrauch & Miller, 2004). This shows that with increasing frequencies, the surfactant concentration needed for the crossover increases. Similarly, for dilatational loss modulus (E''), surfactant bulk concentration initiates two opposing mechanisms. With an increase in bulk concentration, surface concentration also increases resulting in enhanced relaxation between the two phases that facilitates the release of excess surface energy by ST relaxation, thus increasing loss modulus. However, increasing bulk concentration also increases surface's resistance to deformation that decreases

the ST gradient generated by dilatational deformation. This process, on the other hand, results in a reduction in dilatational loss modulus (Z. Huang et al., 2008; Z. Wang, Zhou, et al., 2014). As shown in Fig. 8b., E'' values display a maximum at 0.5% w/v after which it decreases sharply. This indicates that similar to storage modulus, 0.5% w/v makes up the critical limit where one of the opposing mechanisms dominates. For E'', after 0.5% w/v, the decrease in loss modulus related to the decrease in ST gradient becomes more dominant.

The effect of pH and ionic strength on surface rheological properties can be seen in Fig. 8c, d, e, f. Both E' and E'' follow a similar trend, where dilatational modulus displays a local maximum at pH7 and a minimum at a NaCl concentration of 0.3 M. Changes in pH and ionic strength of the medium causes changes in the conformation of polymer chains both at bulk and polymer chains. Bulk conformational changes effect the ease and rate of adsorption whereas surface changes effect properties like equilibrium ST and dilatational modulus (Karbaschi et al., 2014; Kontogiorgos, 2019c). As previously discussed, a thicker and more extensively bonded network on the interface results in increased surface elasticity, which is observed as an increase in dilatational modulus. The effect of molecular conformation on surface rheology was investigated in several studies. Karbaschi et al., 2014 concluded that dilatational modulus values increased for an increasing number of hydrophobic chains exposed to the surface. Additionally, Covis et al., 2014 reported that a more thoroughly unfolded protein chain causes more of the molecule to be adsorbed and increases the length of the loops (non--adsorbed sections of a polymer chain positioned between two points of contact with the interface). With an increasing number of loops, upon surface expansion or compression, non-adsorbed hydrophobic residues could be placed such that they merge with the hydrophobic aggregates within the adsorbed layer and vice versa, therefore reducing the elasticity of the surface and lowering E^* (Covis et al., 2014). The local maxima and minima in these curves presumably represent the points where either of these processes dominates.

4. Conclusion

Quince seed extract, with its chemically complex and diverse structure, is a challenging biopolymer to work with, but has so far shown promising results in stabilization of emulsions and foams. With this study, the objective was to identify the mechanism behind the extract's surface behavior. QSE effectively lowered surface tension at an air-water interface even at concentrations as low as 0.025% w/v (reduction of eq. ST from 72 mN/m to 58.9 mN/m). By QSE addition alone, equilibrium surface tension could be lowered to ~36 mN/m, which is lower than the lowest ST that can be achieved with many other surface-active biopolymers. Critical aggregation concentration (CAC) was identified as 0.165% w/v, which is also lower than similar hydrocolloids, meaning a relatively low extract concentration was sufficient to provide complete surface coverage. *Z*-average particle size data supported this claim by displaying an abrupt increase in mean particle diameter (from ~900 nm to >2500 nm) as bulk QSE concentration exceeds the CAC of 0.165% w/v. Dynamic surface tension curves revealed an almost instantaneous adsorption of polymer for concentrations over 0.01% w/v, which demonstrates the strong potential of the gum as a foaming agent. Surface tension relaxation rates increased with increasing concentration. Dilatational surface rheology measurements revealed that, regardless of concentration, the air-water interface was prominently elastic, implying a high resistance against deformation. Dilatational modulus is highest at a concentration range of 0.3–0.5% w/v for al frequencies investigated. As solution pHs get further from the isoelectric point of QSE proteins, the rate of adsorption of QSE molecules onto the interface and the equilibrium surface pressures increased. Surface properties were also significantly affected by the ionic strength of the medium, with eq. STs decreasing with increasing QSE concentration. pH and ionic strength induced conformational changes in the interfacial layer and also led to local minima and maxima in dilatational elastic and loss modulus within the pH and NaCl concentration studied. Considering these findings, QSE is a very promising natural alternative to other polymeric surfactants and stabilizers currently used in the food, cosmetic and pharmaceutical industries.

Author statement

Emrah Kirtil: Conceptualization, Data curation, Formal analysis, Investigation, Writing - Original Draft, Writing - Review & Editing, Visualization.
Tatyana Svitova: Methodology, Investigation.
Clayton Radke: Supervision, Methodology, Validation.
Mecit Halil Öztop: Supervision.
Serpil Şahin: Supervision.

Declaration of competing interest

The authors declare that they have no known competing financial interests or personal relationships that could have appeared to influence the work reported in this paper.

Acknowledgement

Kirtil E. has received financial support from Fulbright Turkey as part of the Ph.D. Dissertation Research Grant program.

Appendix

In a surface study, identifying the molecular structure is critical because the composition of the interfacial layer is defined by the relative intensities of the many kinds of interactions. These interactions, in turn, are influenced by the specific affinity for the interface and various physicochemical parameters, such as differences in the sizes and shapes, surface activity, overall electrical charges, and hydrophobicity of the molecules (Bos & Van Vliet, 2001; Dickinson, 1999, 2001). Consequently, we believed it would be beneficial to provide the reader with background information on some of the physicochemical properties of quince seed extract.

A.1. Physicochemical Properties of Quince Seed Extract

To best our knowledge, a thorough chemical analysis of the extract is not yet carried out. Thus, we still do not have exact information on the polymer's chemical structure. We have tried to gather pieces of information from different studies and come up with a complete hypothetical molecular model. However, this approach may be prone to some errors. As stated in Phillips (2008), "natural polymers are never uniform or simple; their

functionality depends on more than one structural feature" (Phillips, 2008). The extract is known to be a complex combination of high molecular weight polysaccharides and proteins. Even after a complete analysis of carbohydrate structure, the term "protein" when it is covalently bonded to a polysaccharide, is rather generic and poorly biochemically defined. The information in the literature of the protein fractions concerning their amino acid composition, folding patterns, or physicochemical characteristics currently is insufficient for a complete structural identification (Kontogiorgos, 2019a).

Additionally, the hydrocolloids extracted from fruit seeds are responsible for keeping the seeds moist and enable them to survive in varying climactic conditions (Alizadeh Behbahani et al., 2017; Z.; Huang et al., 2008; Koocheki et al., 2009). Thus, the seed composition is subject to changes depending on the growing conditions, subspecies, age, and other botanical characteristics of the tree as well as harvest season and maturity of the raw material (Buffo et al., 2001). As a result, control of the functionality and reproducibility of the results may be poor. Additionally, the presence of so many unknowns and uncontrollable parameters, introduce an inconsistency that acts as a challenge in interpretation of the results.

A.1.1. Molecular Weight

The weight-average molecular weight of QSE was reported as 9.61×10^6 Da while the number average molecular was reported as 4.153×10^6 Da (Rezagholi et al., 2019), which is greater than wt. av. molecular weight of most common hydrocolloids used in commercial applications; such as Xanthan Gum (2.0×10^6 Da) (Jindal & Singh Khattar, 2018), gum Arabic (7.2×105 Da) (Duvallet et al., 1989), Guar Gum (1.45×10^6 Da) (Khouryieh et al., 2007), Locust bean gum (1.6×10^6 Da) (Doublier & Launay, 1981), Gellan gum (1.64×10^6 g Da) (Sworn & Kasapis, 1998). Though slow to adsorb on the interface, high molecular weight biopolymers can enhance protein foam stability due to their thickening and gelling properties (Rezagholi et al., 2019).

In another study by Wang et al. (2018), the extract was subjected to a two-step purification process in order to remove proteins and any insoluble matter. The researchers have identified three different homogenous fractions of polysaccharides with a Sepharose fast flow column. These carbohydrate fractions, QSG-1, QSG-2, and QSG-3, had average molecular weights of 1250 Da, 1.4×10^6 Da, and 1529 Da, respectively. The major fraction was identified as the one with the highest molecular weight (QSG-2), and further efforts were carried out to map out the molecular structure of this complex polysaccharide (Wang et al., 2018).

A.1.2. Monosaccharide Composition

An analysis of the mucilage itself reveals the presence of the monosaccharides, Xyl, Glc, Ara, Man, Gala, with their relative amounts in this order. Different studies identified different monosaccharide proportions but in almost all Xyl and Glc were the principal monosaccharides (Abbastabar et al., 2015; Hakala et al., 2014; Rezagholi et al., 2019; Vignon & Gey, 1998; L.; Wang et al., 2018). Vignon and Gey (1998) revealed that the mucilage contained Ara, Xyl, Gal and Glc in the proportions 8:54:4:34. Uronic acid content was determined to be 20%. Carboxyl reduction followed by total hydrolysis and GC-MS analysis allowed the identification of the uronic acid as 4-*O*-methylglucuronic acid (Vignon & Gey, 1998). This finding was supported by Lindberg et al. (1990)'s study that showed that the major water-soluble polysaccharide in the mucilage of quince tree seeds is a partially O-acetylated (4-*O*-methyl-d-glucurono)-d-xylan with an exceptionally high proportion of glucuronic acid residues (Lindberg et al., 1990). Rezagholi et al. (2019) also identified Xyl as the most dominant monosaccharide in quince seeed mucilage, followed by Man, Glc and Glca. Thus, the researchers suggested that the gum consisted of a xylan and/or mannon backbone with glucose, galactose, arabinose and glucuronic acid at the branches (Rezagholi et al., 2019; Vignon & Gey, 1998).

Wang et al. (2018) carried out a more detailed analysis and came up with a different model. The three fractions previously mentioned (QSG-1, QSG-2 and QSG-3) exhibited vastly different monosaccharide compositions. QSG-1 and QSG-3 were both rich in glucose and xylose. QSG-3 was especially high in glucose (4.3:0.9 glucose/xylose ratio). So they hypothesized that glucose and xylose were in the backbones of each of these fractions. QSG-2, on the other hand, contained Ara, Glu, Xyl, Gala and Glca in the molar proportion of 4.0:0.3:15.2: 4.2:3.8. Xylose was the most dominant monosaccharide in this large molecule and presumably was present at the backbone.

Even the first study in quince seed mucilage dating back to 1932, reports the presence of celluloses that were not easily separable from the water-soluble gum by dilute acid or alkali treatments at room temperature (Renfrew & Cretcher, 1932). Despite multiple purification steps in other studies, the cellulosic fractions still remained attached to the water-soluble polysaccharides. It was concluded that the strong interactions between cellulose microfibrils and the acidic glucuronoxylan resulted in their coexistence in the mucilage (Ha et al., 1998; Hakala et al., 2014; Vignon & Gey, 1998). Without any purification, Hakala et al. (2014) reported the crude gum extract to be composed of roughly 46% of celluloses and hemicelluloses. This amount was based on the amount of glucose, and considering the fact that water-soluble fractions also contain glucose at the branches (Wang et al., 2018), cellulose content should be less than that under the light of the more recent findings. Cellulosic portions come from the cellulose nanofibrils stored on the epidermal layer of the seeds and have a tendency to self-assemble into a helicoidal organization when dispersed in water (Ha et al., 1998; Hakala et al., 2014; Renfrew & Cretcher, 1932). This attribute assigns the extract a shear-thinning behavior, slippery texture and possible lubrication function, which was also observed in our samples. The smaller MW fractions (QSG-1 and QSG-3) were likely the cellulose and hemicelluloses.

A.1.3. Chemical Structure

When examining the structure as a whole, most studies have found out that the gum was a glucuronoxylan with a very high proportion of glucuronic acid residues (Abbastabar et al., 2015; Lindberg et al., 1990; Ritzoulis et al., 2014; Vignon & Gey, 1998). However, as previously mentioned, the extract is composed of at least three identifiable different homogenous polysaccharide fractions. A detailed chemical structure analysis for separate fractions was only recently carried out by Wang et al. (2018). Thus, here we will try to merge the results of previous studies and reanalyze them under this recent information.

Lindberg et al. (1990) proposed that the extract was composed of a glucan, a galacto-manno-glucan and an acidic arabinoxylan fraction. They claimed that the major water-soluble polysaccharide of quince seed mucilage was partially O-acetylated (4-*O*-methyl-D-glucurono)- D-xylan having an exceptionally high proportion of glucuronic acid residues. Vignon and Gey (1998) found the molar proportions of D-Xyl and 4-*O*-methyl-D-GlcA to be 2:1, and also associated the cellulose microfibrils with a glucuronoxylan possessing high proportions of glucuronic acid residues. All these seem to fit with the findings of Wang et al. (2018).

As previously mentioned, QSG-1 and QSG-3 fractions mainly contained glucose and xylose (with QSG-3 being especially high in glucose). This seems to support the earlier findings that claim cellulose microfibrils were glucuronoxylans (Ritzoulis et al., 2014; Vignon & Gey, 1998). The glucose residues, were present as (1→2)-linked glucopyranosyl uronic acid and (1→4)-linked glucopyranosyl at a molar ratio of 2.2:0.3 (Wang et al., 2018). Thus, QSG-1 and QSG-3 can be identified as cellulose and hemicelluloses composed of glucose, xylose, and glucuronic acid residues at different ratios.

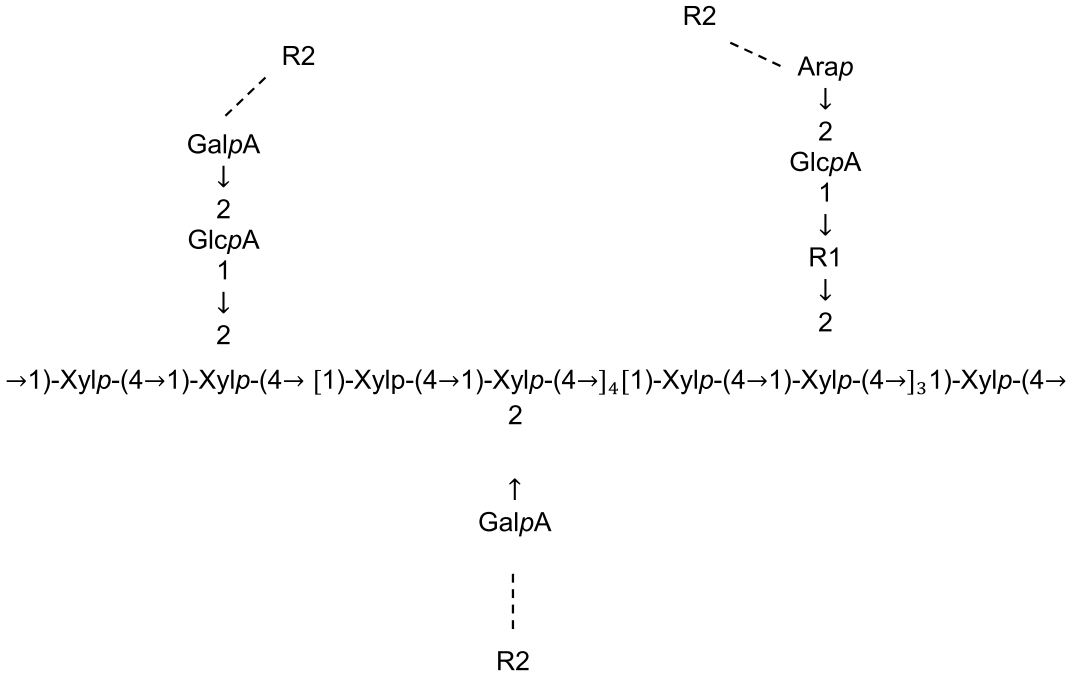

Fig. A1. Proposed structure of QSG-2 (→ : Covalent bonds, - - -: *H*-bonds) (R1: 1, 2, 3, 5-Ara*f* or 1, 4-Glc*p*, R2: NH_2 group of proteins)

The major and bulky proportion (QSG-2) had a more complicated structure. The fraction was very high in xylose (Ara, Glu, Xyl, Gala and GlcA in the molar proportions of 4.0:0.3:15.2:4.2:3.8). The xylose residues were composed of (1/4) and (1→2, 4)-linked xylopyranosyls at a molar ratio of 5.9:4.5. These (1→4) and (1→2, 4)-linked xylopyranosyls residues produced the backbone with branching points at the 2nd position of xylose sugar ring. Quince seed extract had a degree of branching (DB) value of 0.42, which indicates that it is a highly branched molecule (Whistler, 1954, pp. 45–50). This branched structure provides easier hydration related to a higher hydrogen bonding capability. The branches contained 1,2-α-D-GlcpA residues and 1, 2, 3, 5-L-Ara*f*, and were terminated with T-GalpA and T-Ara*p* residues. Considering the results of monosaccharide composition, glycosidic linkage analysis, FTIR spectroscopy, and NMR spectra, the structure of QSG-2 was proposed as shown in Fig. A1 by Wang et al. (2018);

Therefore, overall, QSG-2 a highly branched heteroxylan composed of a (α→4)-β-D-Xyl*p*-(1→2, 4)-β-D-Xyl*p* backbone with 1, 2-α-D-Glc*p*A, 1, 2, 3, 5-L-Araf or 1, 4-β-D-Glc*p* attached to O-2 position forming the side chains. To find the exact positions of uronic acid linkages in the polysaccharide sequence, further attempts are required.

Crude extract contains approximately 20% proteins as determined by our previous study (Kirtil & Oztop, 2016). Proteins are integrated into the gum structure as apparent in its high emulsification and foaming capabilities (Deng et al., 2019; Kirtil & Oztop, 2016). Molecular weight of proteins in QSE ranged between 15 and 60 kDa (Deng et al., 2019). Proteins were, presumably covalently bonded to the extract through the reducing end of the monosaccharides at the ends of the branches (Ara*p* and Gal*p*A) and the amino groups of proteins. Additionally, non-covalent interactions (H-bonding, steric exclusion, electrostatic and hydrophobic) could occur to bind the proteins to the polysaccharide chain. H-bonding, being the strongest among these, can from within polymers containing amide and carbonyl groups in adjacent chains. The partially positively charged hydrogen atoms in N-H groups of one chain can attach to the partially negatively charged oxygen atoms in C=O groups on another (Anal et al., 2019; Reid, 2018). In similar hydrocolloids with surface active properties such as gum Arabic and mesquite gum, proteins are known to be attached to the polysaccharide chain either covalently or non-covalently (Bouyer et al., 2013; Kontogiorgos, 2019a; Vernon-Carter et al., 2008). This indicates that the surface-active fractions of the extract is mostly positioned at the branches. This type of graft co-polymer structure was shown to be highly favorable in emulsion stabilization, which will be discussed further in the upcoming sections (Tadros, 2009).

A.1.4. Amino Acid Composition

Deng et al. (2019) identified the amino acid profile of QSE proteins. CPI contained almost all of the essential amino acids in amounts exceeding that of required by adults as determined by WHO/FAO ("WHO | Protein and amino acid requirements in human nutrition," 2018). The only exception to this was a slight lack of methionine. Glu (26.81%) and Asp (11.45%) were the most abundant amino acids. These amino acids are known to have excellent antioxidant capacities due to the abundance of excess electrons willing to interact with free radicals. Acidic amino acids constitute 38.26% of the whole profile. This coupled with the fact that the seeds also contain organic acids (0.5–0.8 g/kg) such as citric, ascorbic, malic, quinic, shikimic and fumaric acid explains the extract's negative surface charge at neutral pHs (Silva et al., 2005).

What is even more essential and directly related to our study is the exceptionally high amount of hydrophobic amino acids. Hydrophobic amino acids composed 33.27% of the whole amino acid profile, which was higher than that of some other seed proteins such as cumin seed proteins (32.95%) and peony seed proteins (20.87%) (Gao et al., 2017; Siow & Gan, 2014). A higher amount of hydrophobic amino acids provides more sites on the chain that could attach to the interface and is directly related to the polymer's surface activity (Kontogiorgos, 2019a). Basically, for strong adsorption, the molecule needs to be "insoluble" in the dominant medium and has a substantial affinity ("anchoring") to the interface. However, for long term stabilization, the molecule needs to be soluble and be in strong interactions with solvent molecules (Tadros, 2009). So molecules that are composed of sites with both of these two attributes prove to be the most suitable for emulsion and foam stabilization. Considering how soluble the rest of the molecule is, the high hydrophobicity of the proteins is favorable for strong surface adsorption.

Surface hydrophobicity which is associated with the hydrophobic regions exposed at the protein surface is just as essential to surface activity as

hydrophobic amino acid composition. It gives the extent of availability of those hydrophobic regions to the interface (Beverung et al., 1999; Sosa-Herrera et al., 2016). Surface hydrophobicity value of QSE proteins was 932.8 (Deng et al., 2019) which was considerably greater than that of Akebia trifoliata var. australis seed protein isolate (319.4) and Shengzhou I T. grandis seed protein isolate (649) (Du et al., 2012; Yu et al., 2017). This high surface hydrophobicity suggests the presence of unaggregated proteins in the QSE protein dispersion that is responsible for the rapid adsorption on the air/water interface.

Disulfide bonds (SS) and Sulfhydryl groups (SH) are essential functional groups in protein conformation, as they grant structural stability to protein macromolecules and is one of the most dominant protein-protein interaction that influences the proteins' native conformation (Hu et al., 2010). Free SH groups and SS bonds of QSE proteins were found as 9.73 μM/g and 19.79 μM/g, respectively (Deng et al., 2019). This suggests that most of the cysteine exists as disulfide bonds rather than free SH groups. Disulfide bonds are strong covalent bonds that can interconnect the peptide chains in proteins; thus, proteins with more disulfide bonds tend to have a higher resistance against structural disintegration. Presence of disulfide bonds is also associated with a reduced conformational entropy, a tighter and more stable folded structure, and improved thermal stability (Du et al., 2012). A highly stable structure may not be desirable when used for its surfactant properties, since proteins go through a type of denaturation at the interface, unfolding from its native state to expose the hydrophobic regions to the interface (Dickinson, 2018; Karbaschi et al., 2014; Young & Torres, 1989). A higher stability obstructs and extends this procedure.

A.1.5. Other physiochemical properties

QSE has a high charge density compared to some other similar polyelectrolyte biopolymers (such as ghatti and Arabic gums) (Rezagholi et al., 2019). This is associated with the high uronic acid content (20% by wt.) in the form of glucuronic and galacturonic acids (Vignon & Gey, 1998). A thorough analysis by Deng et al., 2019, on the change of extract's zeta potential with pH, indicated that the gum had a maximum positive charge of 26.7 mV at pH 2.0 and a minimum negative charge of −38.1 mV at pH 10. The gum had 0 net charge at pH 4.2, which was accordingly identified as the isoelectric point (Deng et al., 2019). The protein solubility, emulsifying properties and foaming capacity of the gum was found to be directly correlated with the zeta charge of the extract, as observed by the overlapping trend curves of these properties with the zeta potential curve. Protein solubility and emulsifying/foaming capacity of the gum was lowest at its isoelectric point (pH 4.2) and increased at either ends of the pH spectrum. However, basic conditions fortified these properties more than acidic ones, presumably due to the extract's higher content of groups with an affinity towards releasing H+ to the solution, resulting in a higher net negative charge.

QSE yielded relatively good thermal stability, with the thermal degradation starting at 95.1 °C (in the form of protein denaturation). The peak denaturation temperature was reported as 103.4 °C, which is higher than that of many plant proteins (Deng et al., 2019). The strong resistance against denaturation was associated with the high content of disulfide bonds and strong hydrophobic interactions in the protein's native state, as supported by the high hydrophobic amino acid content ($\cong$ 33% *by wt*).

In our previous research, emulsions obtained with QSE and sunflower oil (20% v/v) yielded a typical shear thinning flow behavior with negligible yield stresses (maximum $\tau_0 \leq 1$ *Pa*). The power law index (n) decreased and consistency index (k) increased with increasing concentrations (from 0.05 to 1% w/v), which points out to formation of solutions with higher apparent viscosity and stronger pseudoplastic behavior as concentrations increase (Kirtil & Oztop, 2016). Apparent viscosities also changed with respect to pH, where it was at a maximum around the isoelectric point of pH 4.2 and decreased as you get farther from that to either ends of the pH spectrum (Deng et al., 2019).

References

Abbastabar, B., Azizi, M. H., Adnani, A., & Abbasi, S. (2015). Determining and modeling rheological characteristics of quince seed gum. *Food Hydrocolloids, 43*, 259–264. https://doi.org/10.1016/j.foodhyd.2014.05.026

Adamczyk, Z., Nattich, M., & Barbasz, J. (2009). Deposition of colloid particles at heterogeneous and patterned surfaces. *Advances in Colloid and Interface Science, 147–148*(C), 2–17. https://doi.org/10.1016/j.cis.2008.12.003

Alba, K., Sagis, L. M. C., & Kontogiorgos, V. (2016). Engineering of acidic O/W emulsions with pectin. *Colloids and Surfaces B: Biointerfaces, 145*, 301–308. https://doi.org/10.1016/j.colsurfb.2016.05.016

Alizadeh Behbahani, B., Tabatabaei Yazdi, F., Shahidi, F., Hesarinejad, M. A., Mortazavi, S. A., & Mohebbi, M. (2017). Plantago major seed mucilage: Optimization of extraction and some physicochemical and rheological aspects. *Carbohydrate Polymers, 155*, 68–77. https://doi.org/10.1016/j.carbpol.2016.08.051

Anal, A. K., Shrestha, S., & Sadiq, M. B. (2019). Biopolymeric-based emulsions and their effects during processing, digestibility and bioaccessibility of bioactive compounds in food systems. *Food Hydrocolloids, 87*(August 2018), 691–702. https://doi.org/10.1016/j.foodhyd.2018.09.008

Arabadzhieva, D., Mileva, E., Tchoukov, P., Miller, R., Ravera, F., & Liggieri, L. (2011). Adsorption layer properties and foam film drainage of aqueous solutions of tetraethyleneglycol monododecyl ether. *Colloids and Surfaces A: Physicochemical and Engineering Aspects, 392*(1), 233–241. https://doi.org/10.1016/j.colsurfa.2011.09.061

Ashraf, M. U., Hussain, M. A., Muhammad, G., Haseeb, M. T., Bashir, S., Hussain, S. Z., & Hussain, I. (2017). A superporous and superabsorbent glucuronoxylan hydrogel from quince (Cydonia oblanga): Stimuli responsive swelling, on-off switching and drug release. *International Journal of Biological Macromolecules, 95*, 138–144. https://doi.org/10.1016/j.ijbiomac.2016.11.057

Bantchev, G. B., & Schwartz, D. K. (2003). Surface shear rheology of β-casein layers at the air/solution interface: Formation of a two-dimensional physical gel. *Langmuir, 19*(7), 2673–2682. https://doi.org/10.1021/la0262349

Benjamins, J., Cagna, A., & Lucassen-Reynders, E. H. (1996). Viscoelastic properties of triacylglycerol/water interfaces covered by proteins. *Colloids and Surfaces A: Physicochemical and Engineering Aspects, 114*, 245–254. https://doi.org/10.1016/0927-7757(96)03533-9

Benjamins, J., & van Voorst Vader, F. (1992). The determination of the surface shear properties of adsorbed protein layers. *Colloids and Surfaces*. https://doi.org/10.1016/0166-6622(92)80271-3

Berg, J. C. (2010). *An introduction to interfaces & Colloids: The bridge to Nanoscience*. World Scientific. https://books.google.com/books?id=x-XZBJngdM4C.

Berry, J. D., Neeson, M. J., Dagastine, R. R., Chan, D. Y. C., & Tabor, R. F. (2015). Measurement of surface and interfacial tension using pendant drop tensiometry. *Journal of Colloid and Interface Science, 454*, 226–237. https://doi.org/10.1016/j.jcis.2015.05.012. Academic Press Inc.

Beverung, C. J., Radke, C. J., & Blanch, H. W. (1999). Protein adsorption at the oil/water interface: Characterization of adsorption kinetics by dynamic interfacial tension measurements. *Biophysical Chemistry, 81*(1), 59–80. https://doi.org/10.1016/S0301-4622(99)00082-4

Bos, M. A., & Van Vliet, T. (2001). Interfacial rheological properties of adsorbed protein layers and surfactants: A review. *Advances in Colloid and Interface Science, 91*(3), 437–471. https://doi.org/10.1016/S0001-8686(00)00077-4

Bouyer, E., Mekhloufi, G., Huang, N., Rosilio, V., & Agnely, F. (2013). β-Lactoglobulin, gum Arabic, and xanthan gum for emulsifying sweet almond oil: Formulation and stabilization mechanisms of pharmaceutical emulsions. *Colloids and Surfaces A: Physicochemical and Engineering Aspects, 433*, 77–87. https://doi.org/10.1016/j.colsurfa.2013.04.065

Bouyer, E., Mekhloufi, G., Rosilio, V., Grossiord, J. L., & Agnely, F. (2012). Proteins, polysaccharides, and their complexes used as stabilizers for emulsions: Alternatives to synthetic surfactants in the pharmaceutical field? *International Journal of Pharmaceutics, 436*(1–2), 359–378. https://doi.org/10.1016/j.ijpharm.2012.06.052

Buffo, R. A., Reineccius, G. A., & Oehlert, G. W. (2001). Factors affecting the emulsifying and rheological properties of gum acacia in beverage emulsions. *Food Hydrocolloids, 15*(1), 53–66. https://doi.org/10.1016/S0268-005X(00)00050-3

Bu, H., Kjøniksen, A. L., & Nyström, B. (2004). Rheological characterization of photochemical changes of ethyl(hydroxyethyl)cellulos dissolved in water in the presence of an ionic surfactant and a photosensitizer. *Biomacromolecules, 5*(2), 610–617. https://doi.org/10.1021/bm034443h

Burchard, W. (2001). Structure formation by polysaccharides in concentrated solution. *Biomacromolecules, 2*(2), 342–353. https://doi.org/10.1021/bm0001291

Calero, N., Muñoz, J., Ramírez, P., & Guerrero, A. (2010). Flow behaviour, linear viscoelasticity and surface properties of chitosan aqueous solutions. *Food Hydrocolloids, 24*(6–7), 659–666. https://doi.org/10.1016/j.foodhyd.2010.03.009

Cao, C., Zhang, L., Zhang, X. X., & Du, F. P. (2013). Effect of gum Arabic on the surface tension and surface dilational rheology of trisiloxane surfactant. *Food Hydrocolloids, 30*(1), 456–462. https://doi.org/10.1016/j.foodhyd.2012.07.006

Cascão Pereira, L. G., Johansson, C., Blanch, H. W., & Radke, C. J. (2001). A bike-wheel microcell for measurement of thin-film forces. *Colloids and Surfaces A: Physicochemical and Engineering Aspects, 186*(1–2), 103–111. https://doi.org/10.1016/S0927-7757(01)00488-5

Cascão Pereira, L. G., Théodoly, O., Blanch, H. W., & Radke, C. J. (2003). Dilatational rheology of BSA conformers at the air/water interface. *Langmuir, 19*(6), 2349–2356. https://doi.org/10.1021/la020720e

Castellani, O., Al-Assaf, S., Axelos, M., Phillips, G. O., & Anton, M. (2010). Hydrocolloids with emulsifying capacity. Part 2 - adsorption properties at the n-hexadecane-Water interface. *Food Hydrocolloids, 24*(2–3), 121–130. https://doi.org/10.1016/j.foodhyd.2009.07.006

Castellani, O., Guibert, D., Al-Assaf, S., Axelos, M., Phillips, G. O., & Anton, M. (2010). Hydrocolloids with emulsifying capacity. Part 1 - emulsifying properties and interfacial characteristics of conventional (Acacia Senegal (L.) Willd. var. Senegal) and matured (Acacia (sen) SUPER GUM™) Acacia Senegal. *Food Hydrocolloids, 24*(2–3), 193–199. https://doi.org/10.1016/j.foodhyd.2009.09.005

Chen, M., Feijen, S., Sala, G., Meinders, M. B. J., van Valenberg, H. J. F., van Hooijdonk, A. C. M., & van der Linden, E. (2018). Foam stabilized by large casein micelle aggregates: The effect of aggregate number in foam lamella. *Food Hydrocolloids, 74*, 342–348. https://doi.org/10.1016/j.foodhyd.2017.08.026

Covis, R., Desbrieres, J., Marie, E., & Durand, A. (2014). Dilational rheology of air/water interfaces covered by nonionic amphiphilic polysaccharides. Correlation with stability of oil-in-water emulsions. *Colloids and Surfaces A: Physicochemical and Engineering Aspects, 441*, 312–318. https://doi.org/10.1016/j.colsurfa.2013.09.027

Cserháti, T., Forgács, E., & Oros, G. (2002). Biological activity and environmental impact of anionic surfactants. *Environment International, 28*(5), 337–348. https://doi.org/10.1016/S0160-4120(02)00032-6

Dal-Bó, A. G., Laus, R., Felippe, A. C., Zanette, D., & Minatti, E. (2011). Association of anionic surfactant mixed micelles with hydrophobically modified ethyl (hydroxyethyl)cellulose. *Colloids and Surfaces A: Physicochemical and Engineering Aspects, 380*(1–3), 100–106. https://doi.org/10.1016/j.colsurfa.2011.02.028

Dalgleish, D. G. (2006). Food emulsions - their structures and structure-forming properties. *Food Hydrocolloids, 20*(4), 415–422. https://doi.org/10.1016/j.foodhyd.2005.10.009

Davis, J. P., & Foegeding, E. A. (2006). Foaming and interfacial properties of polymerized whey protein isolate. *Journal of Food Science, 69*(5), C404–C410. https://doi.org/10.1111/j.1365-2621.2004.tb10706.x

Deng, Y., Huang, L., Zhang, C., Xie, P., Cheng, J., Wang, X., & Li, S. (2019). Physicochemical and functional properties of Chinese quince seed protein isolate. *Food Chemistry, 283*(16), 539–548. https://doi.org/10.1016/j.foodchem.2019.01.083

Dickinson, E. (1998). Proteins at interfaces and in emulsions. Stability, rheology and interactions. *Journal of the Chemical Society, Faraday Transactions, 94*(12), 1657–1669. https://doi.org/10.1039/a801167b

Dickinson, E. (1999). Adsorbed protein layers at fluid interfaces: Interactions, structure and surface rheology. *Colloids and Surfaces B: Biointerfaces, 15*(2), 161–176. https://doi.org/10.1016/S0927-7765(99)00042-9. Elsevier.

Dickinson, E. (2001). Milk protein interfacial layers and the relationship to emulsion stability and rheology. *Colloids and Surfaces B: Biointerfaces, 20*(3), 197–210. https://doi.org/10.1016/S0927-7765(00)00204-6. Elsevier.

Dickinson, E. (2003). Hydrocolloids at interfaces and the influence on the properties of dispersed systems. *Food Hydrocolloids, 17*(Issue 1), 25–39. https://doi.org/10.1016/S0268-005X(01)00120-5. Elsevier.

Dickinson, E. (2008a). Interfacial structure and stability of food emulsions as affected by protein-polysaccharide interactions. *Soft Matter, 4*(5), 932–942. https://doi.org/10.1039/b718319d

Dickinson, E. (2008b). Emulsification and emulsion stabilization with protein-polysaccharide complexes. *Gums and Stabilisers for the Food Industry, 14*, 221–232.

Dickinson, E. (2018). Hydrocolloids acting as emulsifying agents – how do they do it? *Food Hydrocolloids, 78*, 2–14. https://doi.org/10.1016/j.foodhyd.2017.01.025

Doublier, J. L., & Launay, B. (1981). Rheology of galactomannan solutions: Comparative study of guar gum and Locust bean gum. *Journal of Texture Studies, 12*(2), 151–172. https://doi.org/10.1111/j.1745-4603.1981.tb01229.x

Du, Y., Jiang, Y., Zhu, X., Xiong, H., Shi, S., Hu, J., Peng, H., Zhou, Q., & Sun, W. (2012). Physicochemical and functional properties of the protein isolate and major fractions prepared from Akebia trifoliata var. australis seed. *Food Chemistry, 133*(3), 923–929. https://doi.org/10.1016/j.foodchem.2012.02.005

Duvallet, S., Fenyo, J. C., & Vandevelde, M. C. (1989). Meaning of molecular weight measurements of gum Arabic. *Polymer Bulletin, 21*.

Effendy, I., & Maibach, H. I. (1995). Surfactants and experimental irritant contact dermatitis. *Contact Dermatitis, 33*(4), 217–225. https://doi.org/10.1111/j.1600-0536.1995.tb00470.x

de Escalada Pla, M. F., Uribe, M., Fissore, E. N., Gerschenson, L. N., & Rojas, A. M. (2010). Influence of the isolation procedure on the characteristics of fiber-rich products obtained from quince wastes. *Journal of Food Engineering, 96*(2), 239–248. https://doi.org/10.1016/j.jfoodeng.2009.07.018

Evans, M., Ratcliffe, I., & Williams, P.a. (2013). Emulsion stabilisation using polysaccharide-protein complexes. *Current Opinion in Colloid & Interface Science, 18*(4), 272–282. https://doi.org/10.1016/j.cocis.2013.04.004

Farahmandfar, R., Asnaashari, M., Salahi, M. R., & Khosravi Rad, T. (2017). Effects of basil seed gum, Cress seed gum and Quince seed gum on the physical, textural and rheological properties of whipped cream. *International Journal of Biological Macromolecules, 98*, 820–828. https://doi.org/10.1016/j.ijbiomac.2017.02.046

Freer, E. M., Svitova, T., & Radke, C. J. (2003). The role of interfacial rheology in reservoir mixed wettability. *Journal of Petroleum Science and Engineering, 39*(1–2), 137–158. https://doi.org/10.1016/S0920-4105(03)00045-7

Freer, E. M., Yim, K. S., Fuller, G. G., & Radke, C. J. (2004a). Interfacial rheology of globular and flexible proteins at the hexadecane/water interface: Comparison of shear and dilatation deformation. *The Journal of Physical Chemistry B, 108*(12), 3835–3844. https://doi.org/10.1021/jp037236k

Freer, E. M., Yim, K. S., Fuller, G. G., & Radke, C. J. (2004b). Shear and dilatational relaxation mechanisms of globular and flexible proteins at the hexadecane/water interface. *Langmuir, 20*(23), 10159–10167. https://doi.org/10.1021/la0485226

Funami, T., Zhang, G., Hiroe, M., Noda, S., Nakauma, M., Asai, I., Cowman, M. K., Al-Assaf, S., & Phillips, G. O. (2007). Effects of the proteinaceous moiety on the emulsifying properties of sugar beet pectin. *Food Hydrocolloids, 21*(8), 1319–1329. https://doi.org/10.1016/j.foodhyd.2006.10.009

Gao, Z., Fang, Y., Cao, Y., Liao, H., Nishinari, K., & Phillips, G. O. (2017). Hydrocolloid-food component interactions. *Food Hydrocolloids, 68*, 149–156. https://doi.org/10.1016/j.foodhyd.2016.08.042

Gonzenbach, U. T., Studart, A. R., Tervoort, E., & Gauckler, L. J. (2007). Macroporous ceramics from particle-stabilized wet foams. *Journal of the American Ceramic Society, 90*(1), 16–22. https://doi.org/10.1111/j.1551-2916.2006.01328.x

Goycoolea, F. M., Calderón De La Barca, A. M., Balderrama, J. R., & Valenzuela, J. R. (1997). Immunological and functional properties of the exudate gum from northwestern Mexican mesquite (Prosopis spp.) in comparison with gum Arabic. *International Journal of Biological Macromolecules, 21*(1–2), 29–36. https://doi.org/10.1016/S0141-8130(97)00037-8

Guzey, D., & McClements, D. J. (2006). Formation, stability and properties of multilayer emulsions for application in the food industry. *Advances in Colloid and Interface Science, 128–130*(2006), 227–248. https://doi.org/10.1016/j.cis.2006.11.021

Ha, M. A., Apperley, D. C., Evans, B. W., Max Huxham, I., Gordon Jardine, W., Viëtor, R. J., Reis, D., Vian, B., & Jarvis, M. C. (1998). Fine structure in cellulose microfibrils: NMR evidence from onion and quince. *The Plant Journal, 16*(2), 183–190. https://doi.org/10.1046/j.1365-313X.1998.00291.x

Hakala, T. J., Saikko, V., Arola, S., Ahlroos, T., Helle, A., Kuosmanen, P., Holmberg, K., Linder, M. B., & Laaksonen, P. (2014). Structural characterization and tribological evaluation of quince seed mucilage. *Tribology International, 77*, 24–31. https://doi.org/10.1016/j.triboint.2014.04.018

Huang, Z., Boubriak, I., Osborne, D. J., Dong, M., & Gutterman, Y. (2008). Possible role of pectin-containing mucilage and dew in repairing embryo DNA of seeds adapted to desert conditions. *Annals of Botany, 101*(2), 277–283. https://doi.org/10.1093/aob/mcm089

Huang, X., Kakuda, Y., & Cui, W. (2001). Hydrocolloids in emulsions: Particle size distribution and interfacial activity. *Food Hydrocolloids, 15*(4–6), 533–542. https://doi.org/10.1016/S0268-005X(01)00091-1

Hu, X. Z., Cheng, Y. Q., Fan, J. F., Lu, Z. H., Yamaki, K., & Li, L. T. (2010). Effects of drying method on physicochemical and functional properties of soy protein isolates. *Journal of Food Processing and Preservation, 34*(3), 520–540. https://doi.org/10.1111/j.1745-4549.2008.00357.x

Isobe, N., Sagawa, N., Ono, Y., Fujisawa, S., Kimura, S., Kinoshita, K., Miuchi, T., Iwata, T., Isogai, A., Nishino, M., & Deguchi, S. (2020). Primary structure of gum Arabic and its dynamics at oil/water interface. *Carbohydrate Polymers, 249*, 116843. https://doi.org/10.1016/j.carbpol.2020.116843

Jindal, N., & Singh Khattar, J. (2018). Microbial polysaccharides in food industry. In *Biopolymers for food design* (pp. 95–123). Elsevier Inc. https://doi.org/10.1016/B978-0-12-811449-0.00004-9.

Karbaschi, M., Lotfi, M., Krägel, J., Javadi, A., Bastani, D., & Miller, R. (2014). Rheology of interfacial layers. *Current Opinion in Colloid & Interface Science, 19*(6), 514–519. https://doi.org/10.1016/j.cocis.2014.08.003

Khouryieh, H. A., Herald, T. J., Aramouni, F., & Alavi, S. (2007). Intrinsic viscosity and viscoelastic properties of xanthan/guar mixtures in dilute solutions: Effect of salt concentration on the polymer interactions. *Food Research International, 40*(7), 883–893. https://doi.org/10.1016/j.foodres.2007.03.001

Kirtil, E., & Oztop, M. H. (2016). Characterization of emulsion stabilization properties of quince seed extract as a new source of hydrocolloid. *Food Research International, 85*. https://doi.org/10.1016/j.foodres.2016.04.019

Kontogiorgos, V. (2019a). Polysaccharides at fluid interfaces of food systems. *Advances in Colloid and Interface Science, 270*, 28–37. https://doi.org/10.1016/j.cis.2019.05.008

Kontogiorgos, V. (2019b). Polysaccharides at fluid interfaces of food systems. In *Advances in colloid and interface science* (Vol. 270, pp. 28–37). Elsevier B.V. https://doi.org/10.1016/j.cis.2019.05.008.

Kontogiorgos, V. (2019c). Polysaccharides at fluid interfaces of food systems. In *Advances in colloid and interface science* (Vol. 270, pp. 28–37). Elsevier B.V. https://doi.org/10.1016/j.cis.2019.05.008.

Koocheki, A., Taherian, A. R., Razavi, S. M. A., & Bostan, A. (2009). Response surface methodology for optimization of extraction yield, viscosity, hue and emulsion stability of mucilage extracted from Lepidium perfoliatum seeds. *Food Hydrocolloids, 23*(8), 2369–2379. https://doi.org/10.1016/j.foodhyd.2009.06.014

Krstonošić, V., Milanović, M., & Dokić, L. (2019). Application of different techniques in the determination of xanthan gum-SDS and xanthan gum-Tween 80 interaction. *Food Hydrocolloids, 87*(July 2018), 108–118. https://doi.org/10.1016/j.foodhyd.2018.07.040

Langevin, D. (2000). Influence of interfacial rheology on foam and emulsion properties. *Advances in Colloid and Interface Science, 88*(1–2), 209–222. https://doi.org/10.1016/S0001-8686(00)00045-2

Liggieri, L., Attolini, V., Ferrari, M., & Ravera, F. (2002). Measurement of the surface dilational viscoelasticity of adsorbed layers with a capillary pressure tensiometer.

Journal of Colloid and Interface Science, 255, 225–235. https://doi.org/10.1006/jcis.2002.8665

Lindberg, B., Mosihuzzaman, M., Nahar, N., Abeysekera, R. M., Brown, R. G., & Willison, J. H. M. (1990). An unusual (4-O-methyl-d-glucurono)-d-xylan isolated from the mucilage of seeds of the quince tree (Cydonia oblonga). *Carbohydrate Research, 207*(2), 307–310. https://doi.org/10.1016/0008-6215(90)84057-2

Liu, Y., Yadav, M. P., & Yin, L. (2018). Enzymatic catalyzed corn fiber gum-bovine serum albumin conjugates: Their interfacial adsorption behaviors in oil-in-water emulsions. *Food Hydrocolloids, 77*, 986–994. https://doi.org/10.1016/j.foodhyd.2017.11.048

Liwarska-Bizukojc, E., Miksch, K., Malachowska-Jutsz, A., & Kalka, J. (2005). Acute toxicity and genotoxicity of five selected anionic and nonionic surfactants. *Chemosphere, 58*(9), 1249–1253. https://doi.org/10.1016/j.chemosphere.2004.10.031

Lucassen, J., & Van Den Tempel, M. (1972a). Dynamic measurements of dilational properties of a liquid interface. *Chemical Engineering Science, 27*(6), 1283–1291. https://doi.org/10.1016/0009-2509(72)80104-0

Lucassen, J., & Van Den Tempel, M. (1972b). Longitudinal waves on visco-elastic surfaces. *Journal of Colloid and Interface Science, 41*(3), 491–498. https://doi.org/10.1016/0021-9797(72)90373-6

Macleod, C. A., & Radke, C. J. (1994). * *I* (Vol. 20, pp. 3555–3566).

Macritchie, F. (1978). Proteins at interfaces. *Advances in Protein Chemistry*. https://doi.org/10.1016/S0065-3233(08)60577-X

Ma, B. D., Zhang, L., Gao, B. Y., Zhang, L., Zhao, S., & Yu, J. Y. (2011). Interfacial dilational rheological property and lamella stability of branched alkyl benzene sulfonates solutions. *Colloid & Polymer Science, 289*(8), 911–918. https://doi.org/10.1007/s00396-011-2415-y

Mendoza, A. J., Guzmán, E., Martínez-Pedrero, F., Ritacco, H., Rubio, R. G., Ortega, F., Starov, V. M., & Miller, R. (2014). Particle laden fluid interfaces: Dynamics and interfacial rheology. *Advances in Colloid and Interface Science, 206*, 303–319. https://doi.org/10.1016/j.cis.2013.10.010

Miller, R., Wüstneck, R., Krägel, J., & Kretzschmar, G. (1996). Dilational and shear rheology of adsorption layers at liquid interfaces. *Colloids and Surfaces A: Physicochemical and Engineering Aspects, 111*(1–2), 75–118. https://doi.org/10.1016/0927-7757(95)03492-7

Möbius, D., Miller, R., & Fainerman, V. B. (2001). *Surfactants: Chemistry, interfacial properties, applications*. Elsevier Science. https://books.google.com.tr/books?id=delDjh2AlTUC.

Moreira, R., Chenlo, F., Silva, C., Torres, M. D., Díaz-Varela, D., Hilliou, L., & Argence, H. (2012). Surface tension and refractive index of guar and tragacanth gums aqueous dispersions at different polymer concentrations, polymer ratios and temperatures. *Food Hydrocolloids, 28*(2), 284–290. https://doi.org/10.1016/j.foodhyd.2012.01.007

Mundi, S., & Aluko, R. E. (2012). Physicochemical and functional properties of kidney bean albumin and globulin protein fractions. *Food Research International*. https://doi.org/10.1016/j.foodres.2012.04.006

Muñoz, J., Rincón, F., Carmen Alfaro, M., Zapata, I., de la Fuente, J., Beltrán, O., & León de Pinto, G. (2007). Rheological properties and surface tension of Acacia tortuosa gum exudate aqueous dispersions. *Carbohydrate Polymers, 70*(2), 198–205. https://doi.org/10.1016/j.carbpol.2007.03.018

Nahringbauer, I. (1995). Dynamic surface tension of aqueous polymer solutions, I: Ethyl (hydroxyethyl)cellulose (BERMOCOLL cst-103). *Journal of Colloid and Interface Science, 176*(2), 318–328. https://doi.org/10.1006/jcis.1995.9961

Orozco-Villafuerte, J., Cruz-Sosa, F., Ponce-Alquicira, E., & Vernon-Carter, E. J. (2003). Mesquite gum: Fractionation and characterization of the gum exuded from Prosopis laevigata obtained from plant tissue culture and from wild trees. *Carbohydrate Polymers, 54*(3), 327–333. https://doi.org/10.1016/S0144-8617(03)00187-5

Pérez-Mosqueda, L. M., Ramírez, P., Alfaro, M. C., Rincón, F., & Muñoz, J. (2013). Surface properties and bulk rheology of Sterculia apetala gum exudate dispersions. *Food Hydrocolloids, 32*(2), 440–446. https://doi.org/10.1016/j.foodhyd.2013.02.007

Phillips, G. O. (2008). Giving nature a helping hand. *Gums and Stabilisers for the Food Industry, 14*, 3–26.

Rakhimov, D. A., Yuldasheva, N. P., Khamidkhozhaev, S. A., & Kondratenko, E. S. (1985). Polysaccharides from the wastes of some fruit and berry, vegetable, and technical crops. *Chemistry of Natural Compounds, 21*(1), 19–21. https://doi.org/10.1007/BF00574241

Ravera, F., Ferrari, M., Santini, E., & Liggieri, L. (2005). Influence of surface processes on the dilational visco-elasticity of surfactant solutions. *Advances in Colloid and Interface Science, 117*(1–3), 75–100. https://doi.org/10.1016/j.cis.2005.06.002

Ravera, F., Loglio, G., & Kovalchuk, V. I. (2010). Interfacial dilational rheology by oscillating bubble/drop methods. *Current Opinion in Colloid & Interface Science, 15*(4), 217–228. https://doi.org/10.1016/j.cocis.2010.04.001. Elsevier.

Ray, A. K., Bird, P. B., Iacobucci, G. A., & Clark, B. C. (1995). Functionality of gum Arabic. Fractionation, characterization and evaluation of gum fractions in citrus oil emulsions and model beverages. *Topics in Catalysis, 9*(2), 123–131. https://doi.org/10.1016/S0268-005X(09)80274-9

Reid, R. (2018). *Inorganic Chemistry*. EDTECH. https://books.google.com.tr/books?id=heLEDwAAQBAJ.

Renfrew, A. G., & Cretcher, L. H. (1932). Quince seed mucilage. *Journal of Biological Chemistry, 97*(1), 503–510. https://doi.org/10.1016/s0016-0032(32)90829-1

Rezagholi, F., Hashemi, S. M. B., Gholamhosseinpour, A., Sherahi, M. H., Hesarinejad, M. A., & Ale, M. T. (2019). Characterizations and rheological study of the purified polysaccharide extracted from quince seeds. *Journal of the Science of Food and Agriculture, 99*(1), 143–151. https://doi.org/10.1002/jsfa.9155

Ritzoulis, C., Marini, E., Aslanidou, A., Georgiadis, N., Karayannakidis, P. D., Koukiotis, C., Filotheou, A., Lousinian, S., & Tzimpilis, E. (2014). Hydrocolloids from quince seed: Extraction, characterization, and study of their emulsifying/stabilizing capacity. *Food Hydrocolloids, 42*, 178–186. https://doi.org/10.1016/j.foodhyd.2014.03.031

Rodríguez Patino, J. M., & Rodríguez Niño, M. R. (1999). Interfacial characteristics of food emulsifiers (proteins and lipids) at the air-water interface. *Colloids and Surfaces B: Biointerfaces, 15*(3–4), 235–252. https://doi.org/10.1016/S0927-7757(99)00012-6

Rub, M. A., Asiri, A. M., Khan, J. M., Khan, R. H., & Din, K.-U. (2013). Interaction of gelatin with promethazine hydrochloride: Conductimetry, tensiometry and circular dichroism studies. *Journal of Molecular Structure, 1050*, 35–42. https://doi.org/10.1016/j.molstruc.2013.07.010

Rühs, P. A., Scheuble, N., Windhab, E. J., & Fischer, P. (2013). Protein adsorption and interfacial rheology interfering in dilatational experiment. *The European Physical Journal - Special Topics, 222*(1), 47–60. https://doi.org/10.1140/epjst/e2013-01825-0

Sanchez, C., Nigen, M., Mejia Tamayo, V., Doco, T., Williams, P., Amine, C., & Renard, D. (2018). Acacia gum: History of the future. *Food Hydrocolloids, 78*, 140–160. https://doi.org/10.1016/j.foodhyd.2017.04.008

Santini, E., Ravera, F., Ferrari, M., Stubenrauch, C., Makievski, A., & Krägel, J. (2007). A surface rheological study of non-ionic surfactants at the water-air interface and the stability of the corresponding thin foam films. *Colloids and Surfaces A: Physicochemical and Engineering Aspects, 298*(1–2), 12–21. https://doi.org/10.1016/j.colsurfa.2006.12.004

Senkel, O., Miller, R., & Fainerman, V. B. (1998). Relaxation studies of surfactant adsorption layers at the liquid/air interface by a funnel method. *Colloids and Surfaces A: Physicochemical and Engineering Aspects, 143*(2–3), 517–528. https://doi.org/10.1016/S0927-7757(98)00586-X

Seta, L., Baldino, N., Gabriele, D., Lupi, F. R., & Cindio, B. de (2014). Rheology and adsorption behaviour of β-casein and β-lactoglobulin mixed layers at the sunflower oil/water interface. *Colloids and Surfaces A: Physicochemical and Engineering Aspects, 441*, 669–677. https://doi.org/10.1016/j.colsurfa.2013.10.041

Shaw, D. J. (1992). *Introduction to colloid and surface Chemistry*. Butterworth-Heinemann. https://books.google.com.tr/books?id=njJCAQAAIAAJ.

Silva, B. M., Andrade, P. B., Ferreres, F., Seabra, R. M., Beatriz, M., Oliveira, P. P., & Ferreira, M. A. (2005). Composition of quince (*Cydonia oblonga* Miller) seeds: Phenolics, organic acids and free amino acids. *Natural Product Research, 19*(3), 275–281. https://doi.org/10.1080/14786410410001714678

Siow, H. L., & Gan, C. Y. (2014). Functional protein from cumin seed (Cuminum cyminum): Optimization and characterization studies. *Food Hydrocolloids, 41*, 178–187. https://doi.org/10.1016/j.foodhyd.2014.04.017

Sosa-Herrera, M. G., Martínez-Padilla, L. P., Delgado-Reyes, V. A., & Torres-Robledo, A. (2016). Effect of agave fructans on bulk and surface properties of sodium caseinate in aqueous media. *Food Hydrocolloids, 60*, 199–205. https://doi.org/10.1016/j.foodhyd.2016.03.033

Stubenrauch, C., & Miller, R. (2004). Stability of foam films and surface rheology: An oscillating bubble study at low frequencies. *Journal of Physical Chemistry B, 108*(20), 6412–6421. https://doi.org/10.1021/jp049694e

Sworn, G., & Kasapis, S. (1998). Effect of conformation and molecular weight of co-solute on the mechanical properties of gellan gum gels. *Food Hydrocolloids, 12*(3), 283–290. https://doi.org/10.1016/S0268-005X(98)00016-2

Tadros, T. (2009). Polymeric surfactants in disperse systems. *Advances in Colloid and Interface Science, 147–148*(C), 281–299. https://doi.org/10.1016/j.cis.2008.10.005

Tadros, T. (2011). Interaction forces between adsorbed polymer layers. *Advances in Colloid and Interface Science, 165*(2), 102–107. https://doi.org/10.1016/j.cis.2011.02.002. Elsevier B.V.

Tang, C. H., Ten, Z., Wang, X. S., & Yang, X. Q. (2006). Physicochemical and functional properties of hemp (Cannabis sativa L.) protein isolate. *Journal of Agricultural and Food Chemistry*. https://doi.org/10.1021/jf0619176

Tcholakova, S., Mitrinova, Z., Golemanov, K., Denkov, N. D., Vethamuthu, M., & Ananthapadmanabhan, K. P. (2011). Control of ostwald ripening by using surfactants with high surface modulus. *Langmuir, 27*(24), 14807–14819. https://doi.org/10.1021/la203952p

Tupy, M. J., Blanch, H. W., & Radke, C. J. (1998). Total internal reflection fluorescence spectrometer to study dynamic adsorption phenomena at liquid/liquid interfaces. *Industrial & Engineering Chemistry Research, 37*(8), 3159–3168. https://doi.org/10.1021/ie9709244

Vereyken, I. J., Chupin, V., Demel, R. A., Smeekens, S. C. M., & De Kruijff, B. (2001). Fructans insert between the headgroups of phospholipids. *Biochimica et Biophysica Acta (BBA) - Biomembranes, 1510*(1–2), 307–320. https://doi.org/10.1016/S0005-2736(00)00363-1

Vernon-Carter, E. J., Pérez-Orozco, J. P., Jiménez-Alvarado, R., Román-Guerrero, A., Orozco-Villafuerte, J., & Cruz-Sosa, F. (2008). Application and evaluation of mesquite gum and its fractions as interfacial film formers and emulsifiers of orange peel-oil. *Food Hydrocolloids, 23*(3), 708–713. https://doi.org/10.1016/j.foodhyd.2008.06.005

Vignon, M. R., & Gey, C. (1998). Isolation, 1H and 13C NMR studies of (4-O-methyl-D-glucurono)-D- xylans from luffa fruit fibres, jute bast fibres and mucilage of quince tree seeds. *Carbohydrate Research, 307*(1–2), 107–111. https://doi.org/10.1016/S0008-6215(98)00002-0

Vrij, A. V. (1976). Polymers at interfaces and the interactions in colloidal dispersions. *Pure and Applied Chemistry*. https://doi.org/10.1351/pac197648040471

Walstra, P. (2002). *Physical Chemistry of foods*. CRC Press. https://books.google.com.tr/books?id=DUsDh-rYif4C.

Walstra, P., & Smulders, P. E. A. (2007). Chapter 2. Emulsion formation. In *Modern Aspects of emulsion science*. https://doi.org/10.1039/9781847551474-00056

Wang, L., Liu, H. M., Xie, A. J., Wang, X. De, Zhu, C. Y., & Qin, G. Y. (2018). Chinese quince (Chaenomeles sinensis) seed gum: Structural characterization. *Food Hydrocolloids, 75*, 237–245. https://doi.org/10.1016/j.foodhyd.2017.08.001

Wang, W., Li, K., Wang, P., Hao, S., & Gong, J. (2014). Effect of interfacial dilational rheology on the breakage of dispersed droplets in a dilute oil-water emulsion. *Colloids and Surfaces A: Physicochemical and Engineering Aspects, 441*, 43–50. https://doi.org/10.1016/j.colsurfa.2013.08.075

Wang, Z. L., Li, Z. Q., Zhang, L., Huang, H. Y., Zhang, L., Zhao, S., & Yu, J. Y. (2011). Dilational properties of sodium 2,5-dialkyl benzene sulfonates at air-water and decane-water interfaces. *Journal of Chemical & Engineering Data, 56*(5), 2393–2398. https://doi.org/10.1021/je1013312

Wang, H. M., Loganathan, D., & Linhardt, R. J. (1991). Determination of the pK(a) of glucuronic acid and the carboxy groups of heparin by 13C-nuclear-magnetic-resonance spectroscopy. *Biochemical Journal*. https://doi.org/10.1042/bj2780689

Wang, Z., Zhou, J., Wang, X. xuan, Zhang, N., Sun, X. xiu, & Ma, Z. su (2014). The effects of ultrasonic/microwave assisted treatment on the water vapor barrier properties of soybean protein isolate-based oleic acid/stearic acid blend edible films. *Food Hydrocolloids*. https://doi.org/10.1016/j.foodhyd.2013.07.006

Ward, A. F. H., & Tordai, L. (1946). Time-dependence of boundary tensions of solutions I. The role of diffusion in time-effects. *The Journal of Chemical Physics, 14*(7), 453–461. https://doi.org/10.1063/1.1724167

Whistler, R. L. (1954). *Guar gum, Locust bean gum, and others* (pp. 45–50). https://doi.org/10.1021/ba-1954-0011.ch008

WHO. (2018). *Protein and amino acid requirements in human nutrition*. WHO.

Wilkins, D. K., Grimshaw, S. B., Receveur, V., Dobson, C. M., Jones, J. A., & Smith, L. J. (1999). Hydrodynamic radii of native and denatured proteins measured by pulse field gradient NMR techniques. *Biochemistry, 38*(50), 16424–16431. https://doi.org/10.1021/bi991765q

Wu, C., Ma, W., Chen, Y., Navicha, W. B., Wu, D., & Du, M. (2019). The water holding capacity and storage modulus of chemical cross-linked soy protein gels directly related to aggregates size. *Lebensmittel-Wissenschaft & Technologie, 103*, 125–130. https://doi.org/10.1016/j.lwt.2018.12.064

Wüstneck, R., Krägel, J., Miller, R., Fainerman, V. B., Wilde, P. J., Sarker, D. K., & Clark, D. C. (1996). Dynamic surface tension and adsorption properties of β-casein and β-lactoglobulin. *Food Hydrocolloids, 10*(4), 395–405. https://doi.org/10.1016/S0268-005X(96)80018-X

Yang, Y., Anvari, M., Pan, C. H., & Chung, D. (2012). Characterisation of interactions between fish gelatin and gum Arabic in aqueous solutions. *Food Chemistry, 135*(2), 555–561. https://doi.org/10.1016/j.foodchem.2012.05.018

Young, S. L., & Torres, J. A. (1989). Xanthan: Effect of molecular conformation on surface tension properties. *Topics in Catalysis, 3*(5), 365–377. https://doi.org/10.1016/S0268-005X(89)80011-6

You, G., Niu, G., Long, H., Zhang, C., & Liu, X. (2020). Elucidation of interactions between gelatin aggregates and hsian-tsao gum in aqueous solutions. *Food Chemistry, 319*, 126532. https://doi.org/10.1016/j.foodchem.2020.126532

Yuan, B., Ritzoulis, C., Wang, X., Pan, W., & Chen, J. (2019). Interactions between mucin and okra gum during pH cycling. *Food Hydrocolloids, 95*, 1–9. https://doi.org/10.1016/j.foodhyd.2019.03.050

Yu, M., Zeng, M., Qin, F., He, Z., & Chen, J. (2017). Physicochemical and functional properties of protein extracts from Torreya grandis seeds. *Food Chemistry, 227*, 453–460. https://doi.org/10.1016/j.foodchem.2017.01.114

Zabiegaj, D., Santini, E., Guzmán, E., Ferrari, M., Liggieri, L., Buscaglia, V., Buscaglia, M. T., Battilana, G., & Ravera, F. (2013). Nanoparticle laden interfacial layers and application to foams and solid foams. *Colloids and Surfaces A: Physicochemical and Engineering Aspects, 438*, 132–140. https://doi.org/10.1016/j.colsurfa.2013.02.046

Zhang, L., Sun, H. Q., Zhang, L., Li, Z. Q., Luo, L., & Zhao, S. (2011). Interfacial dilational rheology related to enhance oil recovery. *Soft Matter, 7*(17), 7601–7611. https://doi.org/10.1039/c1sm05234a. Royal Society of Chemistry.

Zhu, H., & Damodaran, S. (1994). Heat-induced conformational changes in whey protein isolate and its relation to foaming properties. *Journal of Agricultural and Food Chemistry*. https://doi.org/10.1021/jf00040a002